
# BedloadWeb

https://en.bedloadweb.com/

## Concepts and Equations for bedload computation

DOI: 10.13140/RG.2.2.34463.30887

INRAE

OFB
OFFICE FRANÇAIS DE LA BIODIVERSITÉ

Interreg
Alpine Space
HyMoCARES

# CONTENU

# LEXIQUE

| | |
|---|---|
| $A$ | *Cross-section area* |
| $C$ | *Chezy resistance coefficient* |
| $C_f$ | *Bed resistance coefficient* |
| $d$ | *Flow depth* |
| $D$ | *Grain diameter* |
| $D_x$ | *Grain diameter (subscript denotes % finer)* |
| $f$ | *Darcy-Weisbach friction coefficient* |
| $Fr$ | *Froude number* $Fr=U/(gH)^{1/2}$ |
| $F_s$ | *Sand fraction at the bed surface* |
| $k_s$ | *Bed roughness* |
| $n$ | *Manning resistance coefficient* |
| $Q$ | *Flow discharge* |
| $q$ | *Specific discharge* ($q=Q/W$) |
| $Q_s$ | *Sediment discharge at equilibrium flow condition* |
| $q_s$ | *Bedload transport rate per unit width* ($q_s=Q_s/W$) |
| $q_{sv}$ | *Volumetric bedload transport rate per unit width* ($q_{sv}=Q_s/[W\rho_s]$) |
| $R$ | *Hydraulic radius* |
| $Re$ | *Reynolds number* $Re=UR/\nu$ |
| $Re^*$ | *Roughness Reynolds number* $Re^*=u^*D/\nu$ |
| $S$ | *Geometric slope* |
| $S_e$ | *Energy slope* |
| $s$ | *Relative density* ($s=\rho_s/\rho$) |
| $\tan\alpha$ | *Dynamic coefficient of internal friction* |

$U$ *Vertically averaged flow velocity*

$u(z)$ *Mean flow velocity at z level*

$u^*$ *Shear velocity:* $u^* = \sqrt{\tau / \rho}$

$W$ *Channel width*

$z$ *Height above the bed*

$\Phi$ *Dimensionless transport rate:* $\Phi = q_{sv}/[g(s-1)D^3]^{0.5}$

$\kappa$ *Von Karman coefficient (0.4)*

$\rho$ *Fluid density*

$\rho_s$ *Sediment density*

$\tau$ *Bed roughness shear stress [N/m$^2$]*

$\tau'$ *Grain shear stress [N/m$^2$]*

$\tau''$ *Shear stress induced by form resistance [N/m$^2$]*

$\tau^*_c$ *Critical Shields stress corresponding to grain entrainment [ ]*

$\tau^*_m$ *Mobility Shields stress corresponding to the transition from partial to full mobility [ ]*

$\tau^*$ *Shields parameter calculated for diameter $D_x$ [ ]:* $\tau^*_x = \tau/[(\rho_s-\rho)gD_x]$

DOI: 10.13140/RG.2.2.34463.30887 

# 1 ABSTRACT

This document presents the concepts and equations used in the BedloadWeb program. The equations are recalled as they have been presented in the literature. As far as possible the validity domain of each of them is recalled and discussed.

# 2 INTRODUCTION

One of the reasons that motivated the development of BedloadWeb is to make the calculation tools available to as many people as possible through a user-friendly and simplified interface, without having to master the equations of hydraulics and bedload transport. However, many users will want access to these equations (to insert them in a report, to check calculations, to better understand what is calculated ..). This is why this manuscript presents all the equations used in the program.

A question inevitably comes back when using an equation concerns its validity domain. This question is not simple and will be discussed on a case by case basis.

The main steps of a bedload calculation are shown schematically in the following figure:

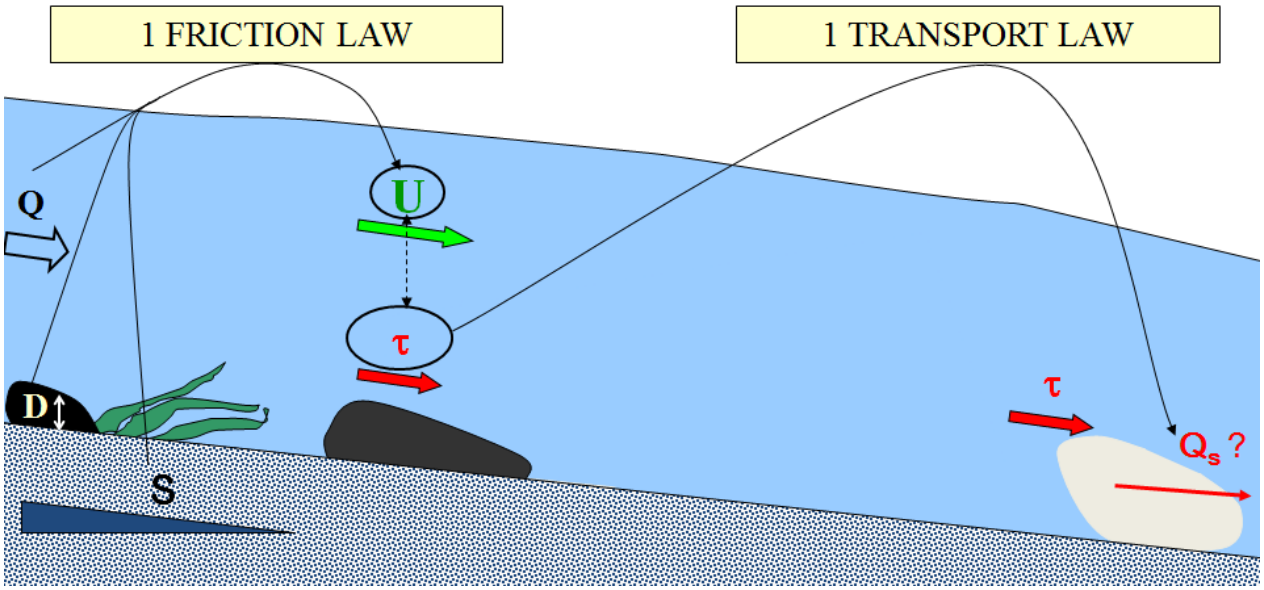


**Figure 1: Schematization of the calculation steps**

First of all, we must define the data necessary for the calculation: granulometry, geometry of the bed and slope, hydrology.

In a second time these data are used to calculate the hydraulic quantities (velocity and water height), via a friction law.

These quantities make it possible to calculate the shear stress (force) exerted on the bed and the bedload transport.

# 3 GRANULOMETRY

## 3.1 The grain size distribution

There are several sediments classes depending on the size:

- Silts : D < 0.02 mm
- Sands : 0.02 < D < 2 mm
- Gravels : 2 < D < 20 mm
- Cobbles : 20 < D < 200 mm
- Boulders : D > 200 mm

But in general sediments are mixtures of different sizes. For example Table 1 shows the bed grain size distribution measured in the Big Wood River, and we can see that all classes are present from sands to boulders (often the whole fine fraction is considered in a single sub-group <2 mm, without distinction between silts and sands)

| D (mm)[1]: | Notation: D (mm) | Fraction $f_i$ | Cumul $\sum f_i$ | Cumul en % |
|---|---|---|---|---|
| 0-2 mm | 2 | 0.070 | 0.070 | 7.0 |
| 2 – 4 mm | 4 | 0.007 | 0.077 | 7.7 |
| 4 – 8 mm | 8 | 0.013 | 0.090 | 9.0 |
| 8 – 16 mm | 16 | 0.037 | 0.127 | 12.7 |
| 16 – 32 mm | 32 | 0.067 | 0.193 | 19.3 |
| 32 – 64 mm | 64 | 0.140 | 0.333 | 33.3 |
| 64 – 128 mm | 128 | 0.213 | 0.547 | 54.7 |
| 128 – 256 mm | 256 | 0.307 | 0.853 | 85.3 |
| 256 – 512 mm | 512 | 0.100 | 0.953 | 95.3 |
| 412 – 1024 mm | 1024 | 0.047 | 1.000 | 100 |

**Table 1**: Bed grain size distribution of the Big Wood river

How to read this table? The first column indicates the size range concerned. In general this column does not appear, but is summarized in column 2: each class is designated by its upper

[1] Important note regarding units: millimeters (mm) are generally used for graphical representations. However, all values must be converted into meters (m) for calculations.

bound. The 3rd column indicates, for each class, the fraction that this class represents in the sediment mixture: number of grains (or mass) in this class divided by the number (or mass) of grain of the sample. The 4th column presents a cumulative distribution, with of course a total equal to 1. The last column is the same with values given in%.

## 3.2 Modeling the bed grain size distribution

The grain size distribution curves is constructed from data [size – Frequency] entered by the user (for example data from a Wolman count).

But BedloadWeb also offers the possibility to model a grain size curve from a knowledge of the $D_{50}$. This may be of interest when only this value is available (which is sometimes the case in study reports), as some transport equations require knowing the whole curve.

There are several ways to model a grain size curve. The literature uses probabilistic laws. However, their use is not easy. The simplest way is certainly to assimilate the grain size curve to a log-normal distribution, whose density function is written:

$$f(D) = \frac{1}{\sqrt{2\pi}\sigma D} exp\left[-\frac{(lnD - \mu)^2}{2\sigma^2}\right] \quad (1)$$

Where μ and σ are the mean and standard deviation for *lnD*. This adjustment can easily be tested on a sample, for example excel using the function LOI.LOGNORMALE.INVERSE.N($f_i$; μ;σ), where $f_i$ ( $0 < f_i$ 1) is the cumulated frequency associated with diameter $D_i$.

Applied to the example of Table 1 this gives μ=4 .56 and σ=1.78. In fact, if the hypothesis of a normal log law is a very practical working hypothesis, in reality the curves are very dysimetric and deviate towards the fine and coarse elements.

The model used in BedloadWeb is based on a similarity analysis of more than 140 curves [*Recking*, 2013b] and is presented in Table 2. It reduces the grain size distribution to 3 parameters: the $D_{50}$, the $D_{84}/D_{50}$ ratio, and the sand content $F_s$ (if there is no sand, the model requires a minimum diameter $D_m$).

| *Di* | *Fi* | ln(Di) | Dcal |
|---|---|---|---|
| 2.0 | 0.070 | 0.69 | 6.9 |
| 8.9 | 0.097 | 2.19 | 9.4 |
| 35.6 | 0.200 | 3.57 | 21.4 |
| 60.4 | 0.296 | 4.10 | 36.9 |
| 87.4 | 0.401 | 4.47 | 61.1 |
| 113.0 | 0.500 | 4.73 | 95.7 |
| 136.4 | 0.600 | 4.92 | 150.4 |
| 173.0 | 0.700 | 5.15 | 243.8 |
| 251.0 | 0.840 | 5.53 | 563.7 |
| 326.3 | 0.900 | 5.79 | 940.6 |
| 627.5 | 0.980 | 6.44 | 3727.6 |
| 1280.1 | 1.000 | 7.15 | 72627.9 |

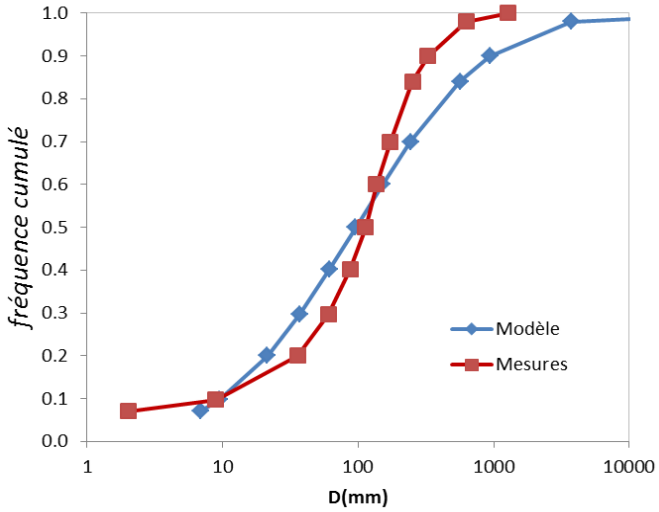


**Figure 2: Modeling of the GSD of the example of Table 1 with a lognormal law.**

| *Class* | *i* (%) | $D_i$ (mm) | $C_n$ |
|---|---|---|---|
| 1 | $100F_s$ | $D_{min}$ (≥2mm) | - |
| 2 | | | 16 |
| 3 | $\frac{50-100F_s}{C_n}+100F_s$ | $\frac{D_{50}-D_{min}}{C_n}+D_{min}$ | 3.3 |
| 4 | | | 1.9 |
| 5 | | | 1.3 |
| 6 | 50 | $D_{50}$ | - |
| 7 | 60 | $\frac{D_{84}-D_{50}}{C_n}+D_{50}$ | 5.9 |
| 8 | 70 | | 2.3 |
| 9 | 84 | $D_{84}$ | - |
| 10 | 90 | | 1.3 |
| 11 | 98 | $C_nD_{84}$ | 2.5 |
| 12 | 100 | | 5.1 |

**Table 2: The bed Grain Size Distribution model. Input data are the sand fraction Fs (or minimum diameter $D_{min}$ if > 2mm), $D_{50}$ and $D_{84}/D_{50}$**

How to use this model?

- The curve is decomposed into 12 classes (column 1).
- Column 2 gives the cumulative percentage of each size class: it is either fixed or calculated from the coefficient Cn given in column 4.
- Column 3 gives the diameters delimiting the upper bound of each class: except for $D_m$ (default 2mm), $D_{50}$, and $D_{84}$ (which are the input data), these values are calculated from the coefficient $C_n$ of column 4.

The model can be easily implemented in Excel; applied with the example of Table 1, it gives with $F_s$ = 0.07, $D_{50}$ = 111.4mm and $D_{84}$ / $D_{50}$ = 2.3:

| Class | *fi*(%) | Di |
|---|---|---|
| 1 | 7 | 2 |
| 2 | 10 | 9 |
| 3 | 20 | 36 |
| 4 | 30 | 60 |
| 5 | 40 | 87 |
| 6 | 50 | 113 |
| 7 | 60 | 136 |
| 8 | 70 | 173 |
| 9 | 84 | 251 |
| 10 | 90 | 326 |
| 11 | 98 | 628 |
| 12 | 100 | 1280 |

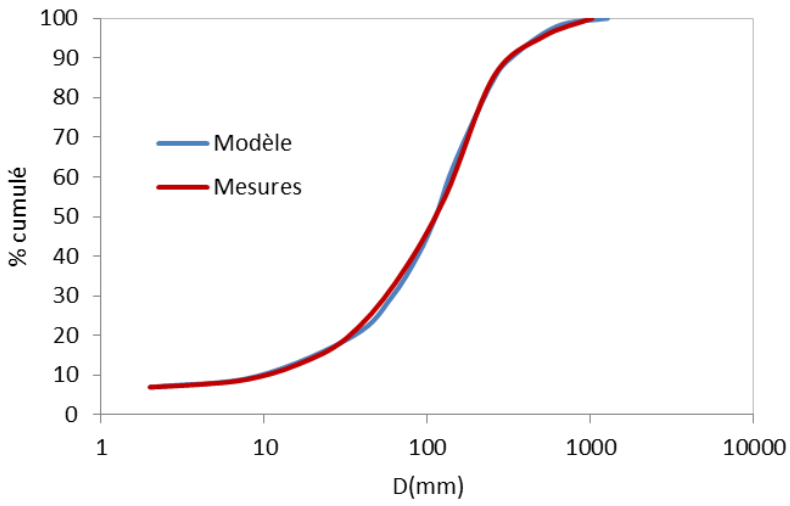


**Figure 3: Modeling of the GSD of** Table 1 **with the similarity model [*Recking*, 2013b].**

This model is very flexible and adapts to almost all forms of grain size curve curves, as shown in Figure 4 where the comparison with 140 grain size curves shows low errors, of the order of a few % at most, whatever the fraction considered.

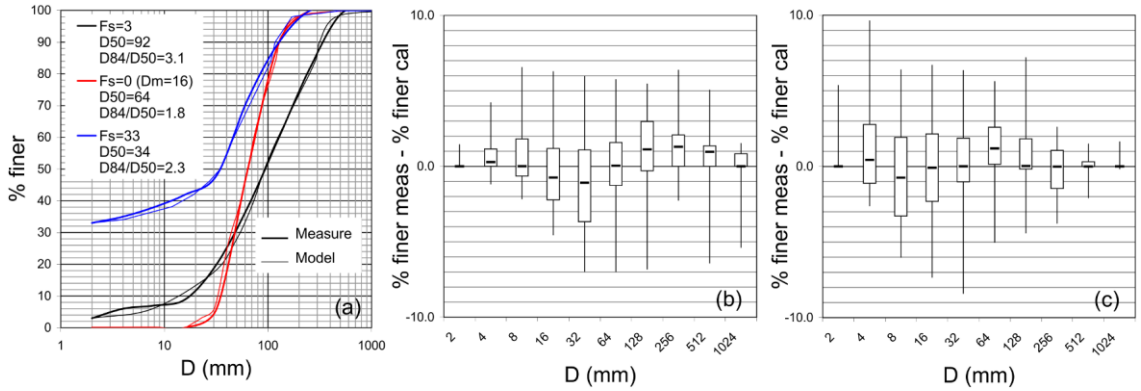


**Figure 4: Modeling of the bed GSD; a) model comparison with 3 GSD and difference between calculated and measured values for b) 78 GSD calibration and c) 43 GSD validation**

The advantage of this model is that we can easily build a very realistic curve from just an estimate of the $D_{50}$, used with the following statistical default values $F_s$ =0.1, $D_{84}/D_{50}$=2 and $D_{90}/D_{84} \approx 1.3$ [*Recking*, 2013b; *Rickenmann and Recking*, 2011]

# 4 HYDRAULICS

## 4.1 Uniform regime

BedloadWeb is not a hydraulics code. It just allows calculating the hydraulics quantities necessary for the quantification of the average bedload transport. All calculations are carried out with the assumption of steady state (constant flow) and uniform (channel with constant geometry and slope, leading to constant hydraulic parameters when moving downstream).

To quantify the average transport rate, we will consider the average hydraulic behavior at the sectional scale. This makes it possible to simplify a succession of complex geometries in a succession of uniform geometries as illustrated in the following figure.

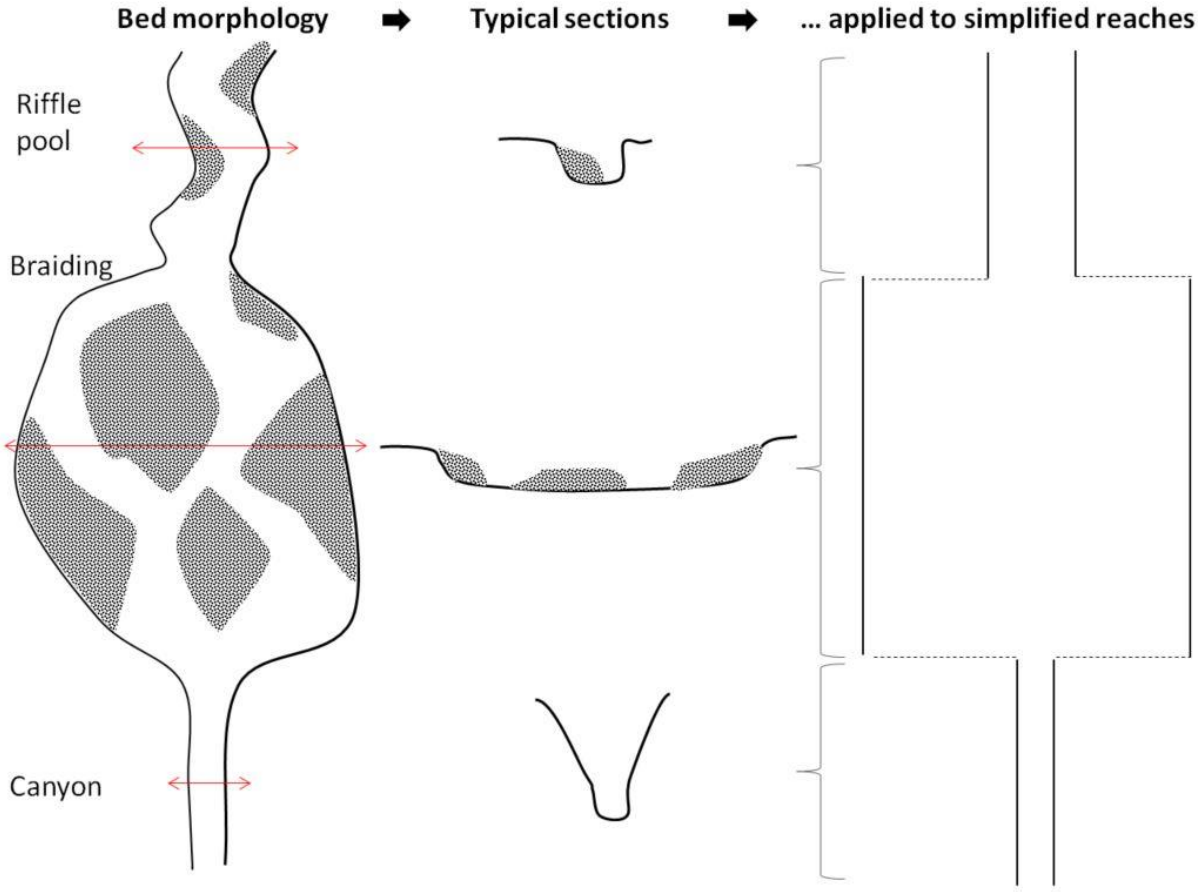


**Figure 5: Approximation of the geometry of the bed by a succession of uniform sections**

For the transient case, the hydrograph is divided into fixed time steps and the permanent uniform calculation is considered for each of these time step.

Calculation in a uniform regime provides a so-called 'normal' water height, ie the height of water generated by the bed friction only (there is no hydraulic wave superimposed on this height). These calculation assumptions would of course be unsuitable for a classical hydraulic study with rapid hydrograph propagation (such as a study of flood risks or hydraulic impacts of a structure), and it will be necessary to implement appropriate hydraulic codes, solving in 1D, 2D or 3D the equations of Saint-Venant or Navier-Stokes according to the complexity of the case treated and the precision sought. Several codes are available online: HEC (Ras https://www.hec.usace.army.mil/software/hec-ras/), Télémac (http://www.opentelemac.org/), Iber (http://www.iberaula.es/)...

# 4.2 Hydraulic radius

It is common to use (for hydraulic calculations) the hydraulics radius *R* (Figure 6), defined by R = A / P (hydraulic section area/ wetted perimeter, defined by the contact between water and the bed). This is motivated by the fact that in narrow sections, the water depth is poorly defined and the water interacts as much with the walls as with the bottom.

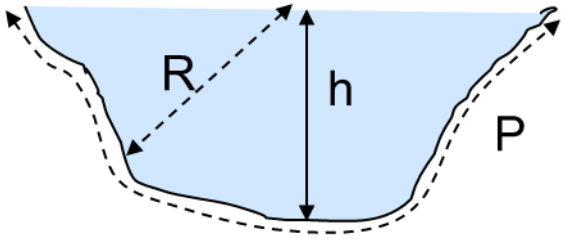


**Figure 6: Schematic representation of the hydraulic radius**

In the BedloadWeb database *R* is indicated for some streams otherwise it is calculated. However, since the geometry is unknown, the hypothesis of a rectangular section (width *W* and depth *d*) is used, which gives $R=Wd/(W+2d)$. In the toolbox, BedloadWeb calculates the hydraulic radius from the section entered by the user.

# 4.3 Froude number

Any flow is the superposition of a mass transfer (volume of water moving with a given velocity U) and a wave propagation (as it would occur after an impact on stagnant water) with a given velocity $\sqrt{gd}$ (where *d* is the water depth and g is the acceleration of gravity). The Froude number Fr is the ratio between these two velocities and is written:

$$Fr = \frac{U}{\sqrt{gd}} \quad (2)$$

When Fr <1, the wave velocity is greater than the flow velocity: the regime is sub-critical and the water height is controlled by the downstream condition (rather characteristic of mild slope rivers). When Fr> 1, the wave is carried away by the current and has no time to propagate. The regime is said hyper-critical, and the water level is controlled by the upstream flow condition (rather characteristic of steep mountain streams).

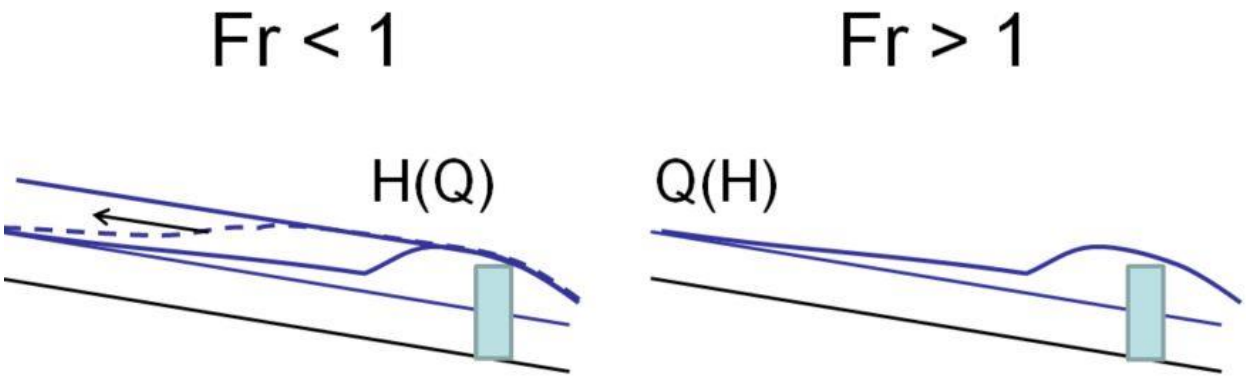


**Figure 7: Impacts of an obstacle introduced into the flow according to the Fr value**

In BedloadWeb the Froude number is given for information because it is not used in the bedload calculations.

# 4.4 Shear stress

## 4.4.1 Définition

The constraint τ (in N/m²) is the force per unit area, i.e. the force F (in Newton) divided by the area on which this force applies (in m²). In Figure 8a $\tau=F/(L\ell)$. For a river section it is the force exerted on the bed by the volume of water flowing in the section divided by the contact surface between the water and the bed (in Figure 8b: length $L_t$ x wetted perimeter P). We call it "shear stress" because this force applies tangentially to the bed.

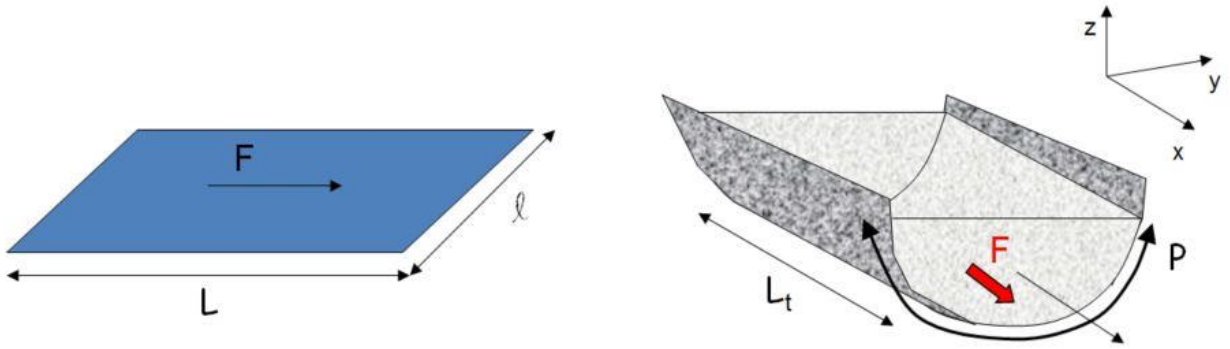


**Figure 8: The bed shear stress**

When considering the weight of water moving in contact with the bed[2], we obtain a simple expression of the bed shear stress that is written:

$$\tau = \rho g d S \qquad (3)$$

Where g is the acceleration of gravity, $\rho$ is the water density, $d$ is the water height (often replaced by the hydraulic radius $R$) and $S$ is the slope.

### 4.4.2 Dimensionless shear stress (or Shields number)

It is common practice in science to use dimensionless quantities. This makes it possible to align on the same graph measurements made under very different experimental conditions (water height, diameters, etc.).

Shields [1936] proposed to adimensionalize the bed shear stress by relating the stabilizing forces (weight) and the destabilizing forces (shear stress τ) acting on a grain placed on the bed; this number is the dimensionless shear stress, or Shields number noted:

$$\tau^* = \frac{\tau}{g(\rho_s - \rho)D} \qquad (4)$$

[2] This formulation is obtained by making a force balance with the assumption of uniform flow regime. The forces involved are the weight of the water P and the friction F. It is assumed that in the uniform regime the two forces compensate each other, which results in the relation ΣF = 0. By projecting on the flow axis this becomes P'-F = 0.

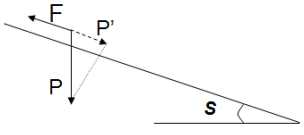


F=P sin(S)≈PS (with sin(S)≈S for mild slopes)

τ x wetted perimeter x length of the reach = water volume x ρgS

$\tau L_t A/R = A L_t \rho g S$ or $\tau = \rho g R S$

Where g is the acceleration of gravity, $\rho$ is the water density, $\rho_s$ the sediment density, $D$ is the grain diameter. It can also be written:

$$\tau^* = \frac{dS}{(s-1)D} \quad (5)$$

Where $s=\rho_s/\rho \approx 2.65$ is the relative density.

### 4.4.3 Bed versus grain shear stress

The water depth $d$ results from all the interactions that can exist between the flow and the bed. This includes interactions with the grains in place on the bed (only this component will interest us for bedload) but also the interactions with the bed geometry (obstacles, narrowing ...) and bedforms. Thus, when the bed shear stress is computed with $d$ in Eq.3, the result may overestimate the force actually really acting on the grains at rest on the bed surface.

Einstein [1950] proposed to decompose linearly the water depth $d$ between a component $d'$ due to friction on the grains composing the bed and a component $d''$ due to the other interactions :

$$d = d' + d'' \quad (6)$$

It permits to writte :

$$\tau = \tau' + \tau'' \quad (7)$$

The shear stress $\tau$ is considered for hydraulics; however only $\tau$' is usually considered for computing bedload transport. We will see in the following how to compute $\tau$'.

## 4.5 Mass conservation

In general, we know the flow rate $Q$ ($m^3/s$) and / or the water depth $d$ (m), and we try to determine the velocity $U$ (m/s). When both $Q$ and $d$ are known, one can easily calculate the velocity with the mass conservation equation:

$$Q = AU \quad (8)$$

Where A ($m^2$) is the flow section. For a rectangular cross section ($A = Wd$) this relation becomes

$$Q = WdU \quad (9)$$

Where $W$(m) is the flow width and $d$(m) is the water depth. But in general we know only $Q$ (or $d$), and we look for $d$ (or $Q$) and $U$. A second equation is required to solve this system with 2 unknowns: this is the friction law.

# 4.6 Friction law

## 4.6.1 Definition

The friction law characterizes the friction exerted by the water on the bed. It relates the flow velocity to the bed characteristics (slope, roughness) and water height (Figure 9). The choice of this law (and its parameters) is essential because it will strongly impact the shear stress computation and therefore bedload computation.

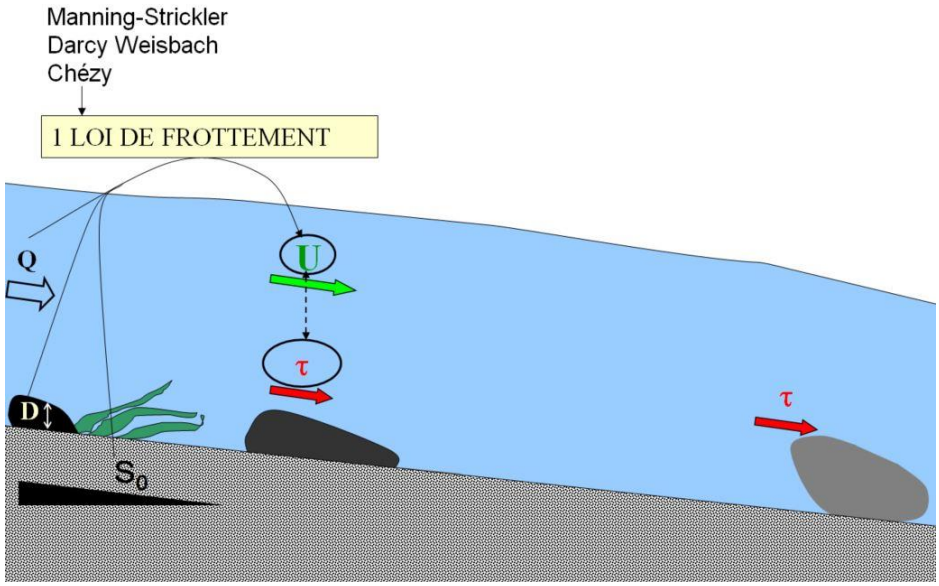


**Figure 9: Schematic representation of how friction laws are used**

We also talk about "flow resistance", because what we are trying to represent is how the roughness of the bed exerts a resistance to the water that flows on its contact. It is easy to imagine, for example, that all other things being equal, the water will flow more easily (higher velocity and smaller depth) on a perfectly smooth surface than on a very rough surface.

## 4.6.2 Near-critical flow hypothesis

Before explaining friction laws in more detail, one can mention a very simple law sometimes used in engineering, and based on the assumption that a mobile bed will adjust its morphology (bed shapes) to minimize the energy required during flooding, so that the Froude number (Eq. 2) will be equal to 1 [*G E Grant*, 1997; *Piton and Recking*, 2019] ; which leads to:

$$U = \sqrt{gd} \tag{10}$$

This simple formulation (not used in BedloadWeb) directly links the flow velocity to the water depth, and its main advantage is that it does not require defining a roughness coefficient.

### 4.6.3 Forces

Fluid mechanics teaches us that any obstacle placed in a fluid flow will develop a force (Figure 10) which will be the result of the pressure exerted by the fluid on the exposed face of the object (effect = push in the direction of the current), but also the depression created behind the object due to the detachment of the current lines in contact with the object (effect = suction in the direction of the current).

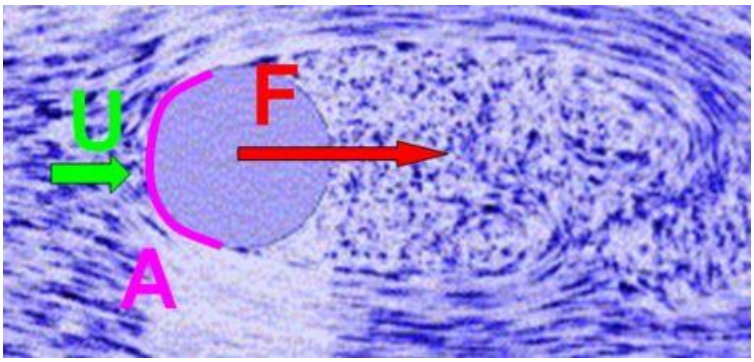


**Figure 10: Drag force**

This « drag » force is written:

$$F = \frac{1}{2}\rho A C_D U^2 \tag{11}$$

Where *U* is the fluid velocity, *A* is the surface of the object exposed to this fluid, and $C_D$ is a coefficient called 'drag coefficient'. This force is exerted by the flow on protruding grains (Figure 11).

**Figure 11: Drag force exerted by the flow on a boulder**

Let extend this concept to the entire riverbed considering not only the isolated pebbles but all obstacles (pebbles, banks, wood, ..) opposing a resistance to the flow as shown in Figure 12.

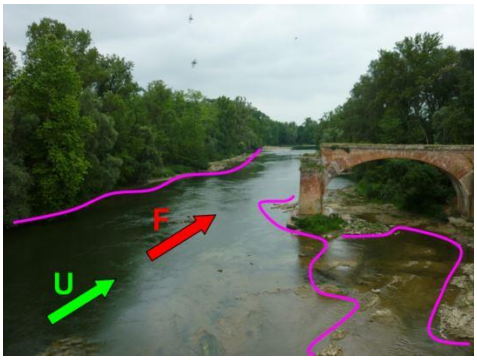


**Figure 12: Drag force exerted by the flow on the river bed**

This force can be written:

$$F = \rho A C_f U^2 \quad (12)$$

where $C_f$=1/2$C_D$ is a friction coefficient. We see here a limit of the exercise since the real impacting surface *A* is very difficult to define. Thus, it is more convenient to define the shear stress $\tau$=*F*/*A* which gives:

$$\tau = \rho C_f U^2 \quad (13)$$

Fluid mechanics introduces another force acting on an object placed within a flow: the lift force. It is due to the pressure gradient created around the object in a shear flow and exerted from below

upwards (Figure 13). This force plays a decisive role in aeronautics. It is recalled here, but is generally not considered for solid transport in the river.

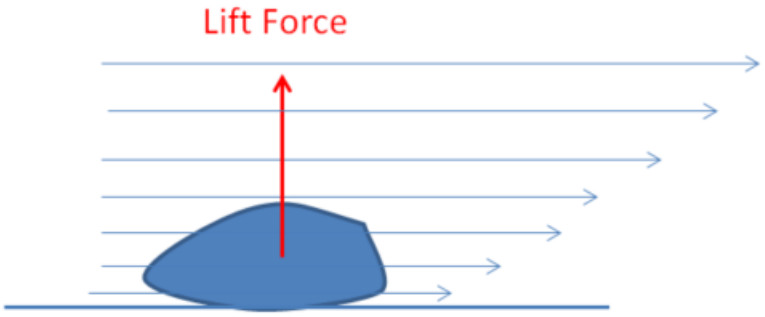


**Figure 13: The lift force in a shear flow**

### 4.6.4 Friction laws

- **Overview**

By matching the two expressions established for shear stress (Eq.3 and 13) we obtain :

$$\rho g d S = \rho C_f U^2 \tag{14}$$

We deduce a friction law which links the flow velocity *U* to the water depth *d* and the bed characteristics (slope *S* and friction coefficient $C_f$):

$$U = \sqrt{\frac{g d S}{C_f}} \tag{15}$$

Which can be written:

$$\frac{U}{u^*} = \sqrt{\frac{1}{C_f}} \tag{16}$$

where $u^* = \sqrt{g d S}$ [m/s] is the 'shear velocity'.

Frictions law from the literature are semi-empirical, but are all variant of Eq. 16 using a different expression for $C_f$. The friction coefficients of Chezy $C$ [$L^{1/2}s^{-1}$], Manning $n$ [$L^{-1/3}s$] (or Strickler $K$=1/$n$) and Darcy-Weisbach $f$ [-], are usually encountered and are linked together and to $C_f$ by the relation :

$$C_f = \frac{g}{C^2} = \frac{gn^2}{h^{1/3}} = \frac{f}{8} \quad (17)$$

For exemple, replacing $C_f$ by the Manning $n$ (ou K=1/n) coefficient in Eq.16, we get:

$$U = \frac{1}{n} h^{2/3} S^{1/2} = K h^{2/3} S^{1/2} \quad (18)$$

It is the Manning-Strickler Equation. The coefficients $n$ or $K$ are often calibrated on observations but one can also use standard values as given in the following example:

| Wall | n (Manning) | K=1/n (Strickler) |
|---|---|---|
| Smooth concrete | 0.01 | 100 |
| Straight canal | 0.025-0.03 | 30-40 |
| Natural stream | 0.03-0.05 | 20-30 |
| Torrent | 0.05-0.1 | 10-20 |
| Torrent with vegetation | >0.1 | <10 |

Tableau 1 : Examples of Manning-Strickler coefficients for different situation

But in gravel beds, most resistance to the flow are produce by friction over the sediment roughness [*Hey*, 1979], and authors have soon proposed to model the Strickler coefficient with the particle diameter [*Strickler*, 1923]:

$$K = \frac{1}{n} = \frac{26}{D_{84}^{1/6}} \quad (19)$$

This kind of formulation gives satisfactory results for streams with a large relative depth d/D> 7 (water depth> 7 x grain diameter), which corresponds more or less to low land rivers, but greatly

overestimates velocities for steep mountain streams with high roughness [*Rickenmann and Recking*, 2011].

The advantage of calibrating a coefficient n or K is that it is very convenient, the calibration taking into account globally all forms of resistance to flow (bed roughness, jams, vegetation, etc.). This is why in BedloadWeb it is suggested to use this friction law for flows in floodplain. For flows inside the main channel, it is recommended to use of a friction law based on the relative height $d/D_{84}$, as explained later.

- **Dimensional analysis**

The left-hand side of Eq.16 is a ratio of two velocities. From a dimensional point of view, this means that we divide [m/s] by [m/s] and that the result is a dimensionless term [-]. We deduce that the right-hand side is also dimensionless and therefore that $C_f$ is dimensionless [-].

Let consider now Eq.17.

If $C_f$ is dimensionless, thus :

- $g/C^2$ is dimensionless, so $C$ has the same dimension as $\sqrt{g}$, that to say [$m^{1/2}/s^{-1}$]
- $gn^2/R^{1/3}$ is dimensionless, so n has the same dimension as $\sqrt{R^{1/3}/g}$ that to say [$s/m^{1/3}$] (and conversely the dimension of $K=1/n$ is [$m^{1/3}/s$])
- $f/8$ is dimensionless, so $f$ is dimensionless

To conclude $n$ (or $K$) and $C$ are dimensional: this conclusion is very important because it means that the values of these coefficients when calibrated for a particular hydraulic condition depend on the conditions for which they were measured (low flows for example) and will not necessarily be valid for other flow conditions (flooding for example).

This is why, for flows in the main channel, many studies have sought a formulation to express the dimensionless coefficient $f$ rather than $n$ or $C$. In general, these formulations are expressed as a function of the relative depth $d/D_{84}$ (in [m] / [m] therefore dimensionless) and remain valid whatever the flow conditions. One main advantage is that formulations established in the laboratory are a priori valid in the field.

- **Friction laws using $d/D_{84}$**

When Manning-Strickler (Eq.18) is used with Eq.19 we get:

$$\frac{U}{u*} = \frac{26}{\sqrt{g}}\left(\frac{h}{D_{84}}\right)^{1/6} \quad (20)$$

But most dimensionless friction coefficients of the literature were obtained with the assumption of a logarithmic velocity profile, which leads to [*Keulegan*, 1938; *Nikuradse*, 1933] :

$$\frac{U}{u*} = 6.25 + 5.75log\left(\frac{h}{k_s}\right) \quad (21)$$

Where $k_s$ is the bed roughness height. The median diameter $D_{50}$ has often been used for $k_s$ [*Keulegan*, 1938], but several authors have preferred $D_{84}$ [*J.C. Bathurst*, 1985] which can be justified by the fact that the turbulence develops around the coarsest elements that emerge from the bed [*Nowell and Church*, 1979; *White*, 1940; *Wiberg and Smith*, 1991].

Actually, in the presence of coarse grain size, it is a multiple of the $D_{84}$ which gives the best results [*Rickenmann and Recking*, 2011], as for example with the law of Hey [*Hey*, 1979] who proposed $k_s=3.5D_{84}$.

But the more one moves towards mountain streams with high roughness and low flow depth (thus weak $h/D_{84}$) the further one moves away from a logarithmic velocity profile and the less efficient these equations are [*Rickenmann and Recking*, 2011]. Actually, the velocity profile develops a roughness layer and deforms until it becomes nearly uniform when the water height is of the order of magnitude of the diameter of the larger grains [*Aberle and Smart*, 2003; *Gimenez-Curto and Cornerio*, 2006; *Lawrence*, 1997; *Nikora et al.*, 2001; *Rickenmann*, 1991].

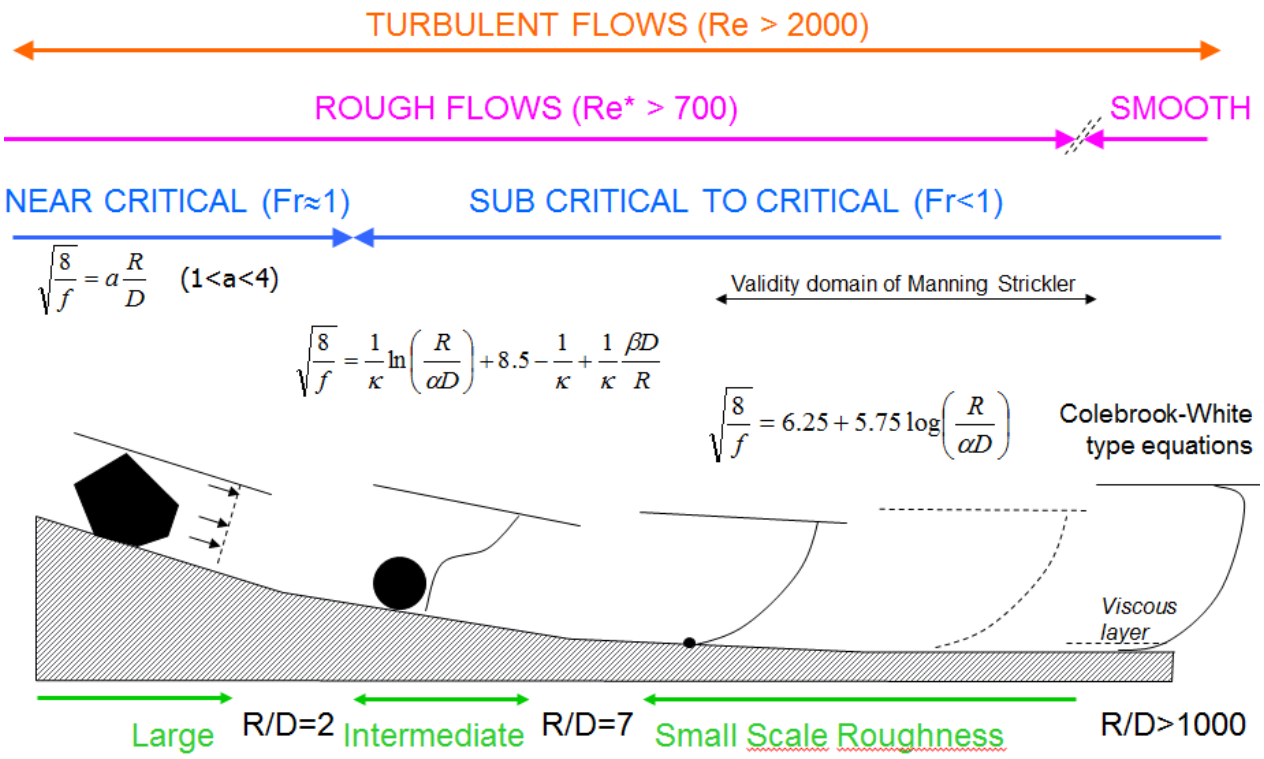


**Figure 14: Variation of hydraulics with the slope**

Ferguson [2007] proposed a relationship providing a transition between the uniform profile at low relative depths and Manning-Strickler for the highest values. Tests carried out on a large field dataset have shown that this relationship is sufficiently powerful to cover all hydraulic configurations encountered from steep mountain slopes to lowland rivers [*Rickenmann and Recking*, 2011]. Ferguson's equation is written:

$$\frac{U}{u^*} = \frac{2.5\,{}^{h}/_{D_{84}}}{\sqrt{1 + 0.15\left({}^{h}/_{D_{84}}\right)^{5/3}}} \qquad (22)$$

This equation is proposed in BedloadWeb.

- **Calculation with *d* or *R* ?**

In BedloadWeb, calculations are done with *R*, even if the comparison with a large dataset [*Rickenmann and Recking*, 2011] shows that the performance of the friction equations is not degraded (and is even slightly better) when velocities are computed with *d* .

- **Calculation with *q***

The above friction laws require to know the water depth *d* (usually replaced by the hydraulic radius *R*), which in the BedloadWeb database is not always the case and where usually only the discharge is known. An option would consist to solve iteratively Eq.22 used with *Q*=*U*/*A* (*A* being the wetted flow section area), but it makes the calculation more complex. This is why BedloadWeb uses an equation directly involving discharge instead of flow depth [*Rickenmann and Recking*, 2011]:

$$\frac{U}{\sqrt{gSD_{84}}} = 1.443q^{*0.6}\left[1+\left(\frac{q^*}{43.78}\right)^{0.8214}\right]^{-0.2435} \quad (23)$$

where $q^* = q/\sqrt{gSD_{84}^3}$ and *q*=*Q*/*L*.

This equation gives results identical to the Ferguson equation when it is used with *d* (and not *R*!). The tests on the large datasets show that it gives very good results in reproducing measured velocities whatever the hydraulic condition considered.

In general, all tests show that predictions are better when using *Q* rather than *d* for hydraulics computation. This is because *d* is difficult to quantify in an irregular section, whereas the flow rate is a finite value if it has been measured correctly and not too far from the velocity measurement section.

A variant (approximation of Eq.23) gives direct access to the water level [*Recking et al.*, 2016] :

$$d = 0.015D_{84}\frac{q^{*2p}}{p^{2.5}} \quad (24)$$

Where *p*=0.24 if *q**< 100 and *p*=0.31 otherwise.

# 4.7 Methods for correcting the shear stress

## 4.7.1 Water depth correction

As mentioned above, only the "grain shear stress" $\tau'$ is a priori interesting for computing bedload transport. Several methods were proposed to calculate this term.

The first method was proposed by Meyer-Peter & Muller [1948]. For a flow characterized by a mean velocity $U$ and a depth $d$, they propose to calculate the fraction $d'$ due to friction on the granular bed with a manning coefficient $n'$ deduced from Eq. 19, which gives:

$$d' = \left(\frac{n'U}{S^{0.5}}\right)^{3/2} \tag{25}$$

By replacing the mean velocity $U$ by the Manning-Strickler equation (Eq.18) we obtain :

$$d' = \left(\frac{n'}{n}\right)^{3/2} d \tag{26}$$

Where the $n$ coefficient is calibrated for the measured flow depth $d$.

To generalize this approach, any friction law $\zeta$ established to express the grain friction only (eg flows over flat bed in the laboratory) can be used with the measured (or computed) flow velocity $U$ to iteratively calculate the water height $d'$ induced by grain friction only.

$$\frac{U}{\sqrt{gd'S}} = \zeta(d'/D) \tag{27}$$

Finally we compute the so called « grain shear stress » $\tau'$ (and the corresponding Shields stress) :

$$\tau' = \rho g h' S \tag{28}$$

In BedloadWeb the Meyer-Peter & Mueller correction is used by default, except when a method is specified with a transport equation.

### 4.7.2 Slope correction

Another approach consists in correcting not the water depth, but the slope *S*. The method (see Rickenmann and Recking [2011] for details) takes into account the energy dissipation induced by strong interactions between the flow and the bed macro-roughness elements, when one moves from low land rivers (fine bed sediments) to mountain streams (boulder streams). The method computes a reduced slope *S'* which excludes the part of the energy slope induced by the local dissipations and not associated with the solid transport process:

$$\frac{S'}{S} = \left(\frac{n'}{n}\right)^e = \left(\sqrt{\frac{f'}{f}}\right)^e \tag{29}$$

Where *S* is the measured (real) slope, *n*' (and *f*') are the Manning (or Darcy) coefficients as they would be computed for the same flow but without macro-roughness (small scale roughness in Figure 14), and *n* (or *f*) are the actual coefficients computed for the flow in question. The *e* coefficient is 1.2-1.5 [*Chiari and Rickenmann*, 2010].

In BedloadWeb the corrected slope *S'* is calculated with [*Rickenmann*, 2012]:

$$\sqrt{\frac{f'}{f}} = \left(\frac{U(q)}{U'(q)}\right)^{1.5} \tag{30}$$

Where $U(q)$ is the mean flow velocity (Ferguson or Eq. 23) and $U'(q)$ is the velocity calculated with the equation characterizing the' base flow resistance ', in the absence of macro-roughness [*Rickenmann and Recking*, 2011]:

$$U'(q) = 3.074\sqrt{gSD_{84}}q^{*0.4} \tag{31}$$

### 4.7.3 Shields correction

A transport equation presented below [*Recking*, 2013a] does not use any shear stress correction. This equation has the particularity to use the $D_{84}$ as a characteristic diameter (unlike all the other equations that use the median or average diameter) which does not impact the shears stress value,

but the Shields number (Eq.4) : because $D_{84} \approx 2D_{50}$ in general, the Shields number is reduced accordingly by half.

Figure 15 compares for the BedloadWeb database ($10000^{+}$ values), the Shields numbers calculated with $\tau'$ (corrected by the Meyer-Peter & Muller method) and $D_{50}$, and the Shields numbers calculated with $\tau$ (no correction) and $D_{84}$. It can be seen that the two approaches give fairly comparable results.

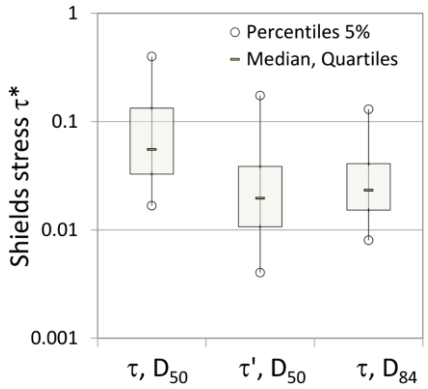


**Figure 15: Shields numbers calculated for a large database (> 10000 values) a) without shear stress correction and $D_{50}$ b) with the MPM correction and $D_{50}$ c) without shear stress correction and $D_{84}$**

# 5 INITIATION OF MOTION

## 5.1 The concept of beginning of transport

The concept of beginning of transport is both important and complex. Important because it provides information on a river functioning (for the ecological diagnosis, the stability of structures...), but also because it is a central parameter in many bedload equations. Complex because its definition is not clearly established: when should one consider that transport exits? The complexity of sediment mixtures makes it difficult to consider as a whole the behavior of each class of grains, which led to many results sometimes very different when trying measure threshold transport [*Buffington and Montgomery*, 1997].

In the laboratory, with uniform materials, the beginning of transport was associated with the first grain movement when the flow is increased. In the field, the 'competent flows' method consists of associating the largest mobilized grain size *D* (generally deduced by observation of the bed after the flood) to a maximum shear stress exerted by the flow in question [*Andrews*, 1983; *Petit*, 1994; *A C Whitaker and D F Potts*, 2007].

## 5.2 Critical $\tau_c$* and reference $\tau_r$* Shields stress

The theoretical development about beginning of transport can be traced back to Shields [1936], and are still widely used today.

Shields performed a series of laboratory experiments to observe the motion of different materials and produced the following curve known as the "Shields Curve". The X axis shows the particle Reynolds number Re* which is a characterization of the flow regime (we will not explain it here, remember that in natural rivers Re *> 1000 approximately). The Y axis shows the corresponding values for $\tau$*. The curve represents the boundary between the conditions maintaining the grains at rest (below) and the conditions where mobility is observed (above), and thus represents the critical threshold for motion; the values of $\tau$* located on this curve are the critical Shields numbers $\tau_c$* for the different flow conditions:

$$\tau_c^* = \frac{d_c S}{(s-1)D} \quad (32)$$

Where $d_c$ is the critical flow depth for initiation of motion.

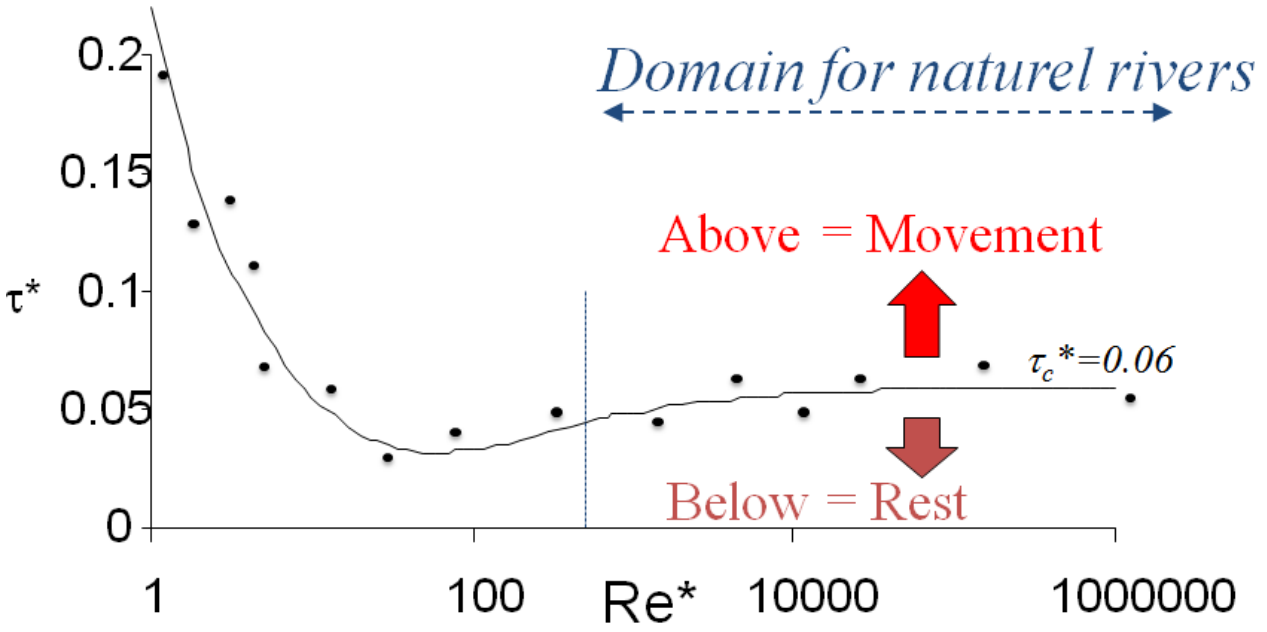


**Figure 16: The Shields curve (points are given for illustration, but are not the real values)**

One of the interesting point of the Shields results is that the curve seems to converge towards a constant value $\tau_c$*=0.06 when Re*>1000 (that is to say for the conditions that prevail in rivers).

The critical Shields stress concept is confronted with the difficulty of defining the threshold of motion (movement of a grain - of a group of grain - of what size?). This is why, as an alternative to the critical Shields stress, other authors proposed a reference Shields stress which is the Shields stress value associated with a small and finite transport rate, regardless of the diameter concerned [*G. Parker et al.*, 1982; *P Wilcock*, 2001]. They define a dimensionless transport W *:

$$W^* = \frac{(s-1)gq_v}{\rho_s u_*^3} \qquad (33)$$

Where $q_v$ [m3/s/m] is a volumetric transport per unit width and $u_* = \sqrt{ghS}$ is the shear velocity. The peculiarity of this term is that it does not involve the grain diameter (a parameter that is difficult to define for a grain size distribution), unlike Einstein parameter (dimensionless solid discharge) $\Phi = q_v/\sqrt{g(s-1)D^3}$, which is used by most bedload equations (see below). The reference constraint $\tau_r$ is defined as the value of $\tau$ for which *W** is equal to a reference value, which has been fixed arbitrarily at *W** = 0.002 [*G. Parker et al.*, 1982].

In the following, the beginning of movement will be designated by $\tau_c$* or $\tau_r$*.

## 5.3 Which value for $\tau_c^*$ ?

The value $\tau_c^* = 0.06$ has long been used as a reference but since Shields many authors have proposed different values [*Buffington and Montgomery*, 1997]. For instance Meyer-Peter et Muller [1948] used $\tau_c^*=0.047$, and Parker et al [2003] proposed $\tau_c^*=0.03$.

Recent studies based on both laboratory experiments and field measurements suggest that this parameter may actually change with slope [*Lamb et al.*, 2008; *Mueller and Pitlick*, 2005; *Recking*, 2009; *Recking et al.*, 2008]. For instance Lamb et al [2008] proposed :

$$\tau_c^* = 0.15S^{0.25} \quad (34)$$

A slightly different version [*Recking et al.*, 2008] using an exponent 0.275 instead of 0.25 is used for displaying graphics in BedloadWeb (when $\tau^*/\tau_c^*$ is used in X axes). In the display options the user has the possibility to change the $\tau_c^*$ value as well as the percentile of the particle size distribution to which it applies (because $\tau_c^*$ must apply to a grain diameter as indicated by Eq.4 ; by default, the median diameter $D_{50}$ is used).

For bedload computation, the defaults values are those specified with the transport equation, but the user also has the option of setting this parameter.

## 5.4 Hiding effects

The concept of beginning of movement is relatively simple to understand if we consider a sediment mixture comprising a single diameter (uniform material), but what about complex sedimentary mixture?

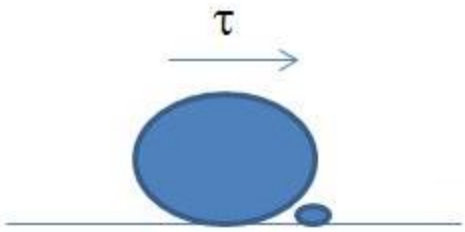


**Figure 17: Hiding and overexposure; which of the largest or the smallest will be more likely to be mobilized by the flow? The smallest because of its size? The largest because of his exposure? or both because when the largest moves the smallest are exposed (equivalent mobility)?**

One could say as a first approximation that for a given shear stress, a grain of sand will be more mobile than a pebble. However the example of Figure 17 suggests that it is not so simple for example if this grain of sand is hidden behind the pebble and is thus protected from the flow. This notion has been conceptualized as 'hiding and exposure' [*Egiazaroff*, 1965; *Einstein and Chien*, 1953]. It is generally modeled with a formulation taking the following form [*G. Parker and Klingeman*, 1982] :

$$\tau_{ci}^{*} = \tau_{c50}^{*}\left(\frac{D_i}{D_{50}}\right)^{\alpha} \quad (35)$$

where α is a coefficient whose value is 0 if the critical shear stress is simply proportional to individual particle size (constant critical Shields value) or –1 in case of complete equal mobility. Equal mobility could be verified both in the field and in the experimental channel and proved to be a good approximation in some cases [*Andrews and Parker*, 1987; *Kuhnle*, 1992; *G. Parker and Klingeman*, 1982; *Wiberg and Smith*, 1987; *P.R. Wilcock*, 1993], while other studies describe rather significant selective transport of fine sediment [*Ashworth and Ferguson*, 1989; *Komar*, 1987; *Lanzoni*, 2000; *Lisle*, 1995]. So there is still very strong uncertainties about this the value of α (values were generally proposed between –0.6 and –1). Nevertheless, an adjustment of the available data (laboratory and field) led to the following formulation for diameter $D_{84}$ [*Recking*, 2009] :

$$\tau_{c84}^{*} = 0.56S + 0.021 \quad (36)$$

In BedloadWeb this relation is used with the GTM model for the calculation of the bedload grain size distribution (see § at the end of this document).

# 5.5 The critical Shields number in practice

- **Calculation of $d_c$ or $q_c$**

Knowing the value of $\tau_c$* an immediate way to use the critical Shields stress is to calculate the critical water depth for which a grain of diameter *D* will be set in motion:

$$d_c = \frac{1.65D}{S}\tau_c^{*} \quad (37)$$

In this formulation, $\tau_c$* can take a fixed value or be calculated from the slope (Eq.32 or 36 for example). By replacing $d_c$ in a friction equation (Eq.22 for instance) one can deduce a critical velocity $U_c$, and the critical discharge for the beginning of transport is calculated with:

$$q_c = h_c * U_c \quad (38)$$

- **Calculation of bed stability**

Conversely, what is the minimum diameter that will have to be used for the bed to remain stable up to a given design water level (rip-rap calculation for example)?

$$\mathrm{D}_{min} = \frac{h_{projet} S}{1.65 \tau_c^*} \quad (39)$$

For rip-rap design the choice of the $\tau_c$* value must be carefully considered so as not to oversize the blocks [*Recking and Pitlick*, 2013].

# 6 BEDLOAD EQUATIONS

## 6.1 Overview

The equations used in BedloadWeb are described one by one in this part. For each of them we will try to give a maximum of information, as for example the conditions of establishment of the formula, the field of validity ... But before presenting the formulas it is important to bring some clarifications on the basic concepts underlying the development and use of such tools.

### 6.1.1 What is a bedload equation ?

Most equations are semi-empirical, that is to say that they are based on a more or less elaborate theoretical basis, the parameters of which are calibrated on experimental datasets. They usually relate a dimensionless parameter characterizing hydraulics to a dimensionless parameter characterizing transport. The usual parameters are:

- the Shields number (Eq.4)
- the dimensionless transport W* (Eq. 33)
- the Einstein parameter Φ

$$\Phi = \frac{q_v}{\sqrt{g(s-1)D^3}} \tag{40}$$

Using dimensionless parameters generally reduces the dispersion due to experimental conditions and aligns the points on a relationship that we hope will be unique:

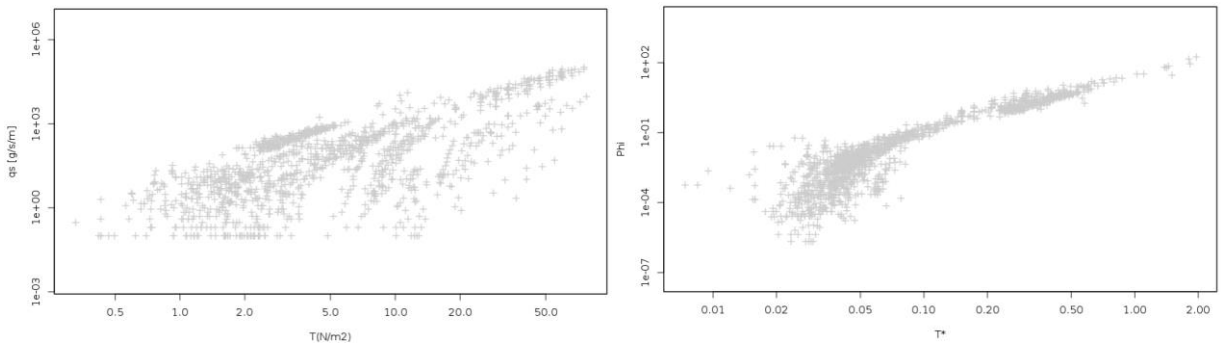


**Figure 18: Adimensionalization of the flume data on BedloadWeb**

To be short, we will distinguish two families of equations; threshold formulas that will be of the form:

$$\Phi = f(\tau^* - \tau_c^*) \quad (41)$$

And transport stage equations (with no threshold) given in the form:

$$\Phi = f(\tau^*/\tau_c^*) \quad (42)$$

The threshold equations have the particularity that transport is zero when $\tau^* < \tau_c^*$, what render the choice of $\tau_c^*$ delicate. Transport stage equations use the ratio $\tau^*/\tau_c^*$ and are less restrictive because they predict a (weak) transport even when $\tau^*$ vanishes to zero.

### 6.1.2 Validity domain

Knowing the validity domain of any equation is crucial for practical use, and it is far from trivial for bedload equations because it was often not specified by their authors.

As a consequence, the conditions of establishment of the equations (lab or field, granulometric range) is sometime considered as validity domain. This is false because one of the first objectives when adimensionalizing parameters is precisely to make the equation independent from the experimental conditions from which they were established.

For instance, for a given slope, a low water depth $h_s$ will be required for transporting sands with small diameter $D_s$, whereas a higher water height $h_g$ will be required to mobilize gravel and pebbles of larger diameter $D_g$. But the two flows can have the same ratios $h_s/D_s = h_g/D_g$ and thus the same Shields number (Eq.4). In addition, a flow similarity between the flume and the field is usually respected by working with the same Froude number (Froude similarity).

But beside these theoretical considerations, there are fundamental differences between the laboratory and the field, which questions the possibility of using in the field formulations established in the laboratory.

### 6.1.3 Laboratory or field

Equations can be classified in two main categories: those resulting from flume data, and those resulting from field data; but some equations have a mixed origin.

All field and laboratory data can be viewed in BedloadWeb.

| Paramter | Flume data | Field data |
|---|---|---|
| Slope (m/m) | 0.001–0.2 | 0.00004–0.10 |
| $D_{50}$ (mm) | 0.3-44.3 | 0.25-220 |
| $D_{84}$ (mm) | --- | 0.3-558 |
| Bankfull depth (m) | --- | 0.04-7.5 |
| Bankfull width (m) | 0.05-2 | 0.3-578 |
| Nomber of values | 1244 | 10028 |

**Tableau 2: Summary of the flume and field data available in bedloadWed**

A summary of some of the flume experimental conditions is given in appendix.

| | Laboratory | Field | Question |
|---|---|---|---|
| Granulometry | The materials used are uniform or nearly uniform | Grain size distributions are very heterogeneous | Part of the field complexity is poorly represented in the lab, such as hiding effects |
| Granulometry | The material transported and those present on the bed surface are usually the same (uniform particle size) | The materials transported are usually very different from those present on the bed surface. | Can we use a flume derived equation in the field with the bed GSD (only available) as an input? |
| Equilibrium | Many experiments have considered transport rates for equilibrium condition, i.e. with a constant slope, when the flume input solid discharge is equal to the flume output solid discharge. | Field bedload measurements were carried out on various sections without any possibility of controlling any equilibrium condition for the sections in question. | Equilibrium is not guaranteed in the field (and probably never verified): are flume derived equations developed to describe this state systematically out of their validity domain in the field? |
| Section | The flow is almost 1D because constrained between the two vertical walls of the (generally) narrow flume, with almost no lateral variability. | Each measurement results from samples collected at different location in the complex section and averaged over the section. As a consequence, the natural variability of the section (and its eventual impact on the process of transport) is present in the data. | Bedload transport is a strongly non-linear response to shear stress and is therefore sensitive to water level variations on the section. Results will necessarily differ when section averaged hydraulic quantities are used with bedload equation calibrated with 1D averaged (field) or 1D local (flume) data. Same question arises when local data (2D) are used with these equations. |

These fundamental differences between field and laboratory data strongly impact the derived bedload equations. Each point is discussed again later.

The validity domain of an equation is therefore difficult to define and will remain uncertain in any case. One way to cope with these uncertainties will be to test the equations on a restricted dataset that matches the characteristics (slope, grain size, morphology) of the case studied. This is possible from the database in BedloadWeb.

### 6.1.4 Transport at capacity

Many flume derived equations have been established for the equilibrium condition (steady state condition where the input equals the output solid discharge). When this condition is verified, the transport is said at capacity. In the opposite case we distinguish:

- The flow is said to be 'supply limited' when the equation overestimates the transport rate: it is considered that compared to the reference equilibrium condition, the bed sediments available for transport are insufficient for the given hydraulic condition (Shields number);
- The flow is said 'transport limited' when the equation underestimates bedload: it is considered that compared to the reference equilibrium condition, the hydraulic conditions are not strong enough to mobilize the bed in place (characterized by its slope and granulometry)

This argument is often used to justify that a calculation gives poor results; perhaps a bit too hastily because there are plenty of reasons that can justify over or underestimation (starting with uncertainties of the input data used in the models, but also uncertainties of the measured solid discharge used for comparison). In addition, we will see later that this notion of equilibrium no longer makes sense when an equation is constructed from data measured in the field, for which no equilibrium condition is verified.

But whatever the measurements quality, the definition of the particle size to be used in the equations when a poorly graded natural grain size distribution (mixture of several diameters) must be used in place of the uniform flume material (a single diameter) remains an unresolved central problem that can largely explains over or under-prediction.

### 6.1.5 Fractional calculation

Most flume experiments considered a single diameter $D$ (uniform mixture), and equations derived from these experiments are usually used in the field with the median diameter $D_{50}$, assuming that it is representative for the whole sediment mixture.

It is (to the best of my knowledge) Parker et al [*G. Parker and Klingeman*, 1982; *G. Parker et al.*, 1982] who first adapt equations to the complexity of the field, with a better consideration for the bed grain size distribution. They proposed a fractional calculation, which consists of calculating the transport rate not for a representative single diameter, but for all the particle size classes present in the bed grain size distribution.

Let consider a transport equation $\zeta$ established for a characteristic grain diameter $D$, as a function of the shear stress $\tau$ and critical shear stress $\tau_c$ (in general the reference stress $\tau_r$ has been used in this type of formulation):

$$q_s = \zeta(D, \tau, \tau_r) \quad (43)$$

Fractional calculation assumes that the function $\zeta$ remains valid for each particle size class $D_i$ present in the bed sediment mixture, which makes it possible to write:

$$q_{si} = f_i \zeta(D_i, \tau, \tau_{ri}) \quad (44)$$

Where $f_i$ is the proportion of material present in the i$^{th}$ size class of the sedimentary mixture (the curve is divided into intervals [$D_i$-$D_{i+1}$]), $\tau_{ri}$ is the reference shear stress associated with the size $D_i$, and $q_{si}$ is the solid discharge associated with this diameter. The value of $\tau_{ri}$ is generally expressed as a function of $\tau_{r50}$ (estimated for the median diameter $D_{50}$) from a hiding function (Eq. 35).

The total solid discharge $q_s$ is then the sum of the solid discharge $q_{si}$ calculated for each class:

$$q_s = \sum q_{si} \quad (45)$$

This type of decomposition is well adapted to equations in the form $\tau$-$\tau_c$ but gives inconsistencies for the equations written with $\tau^*/\tau_c^*$ (the fractional calculation $\sum f_i \zeta(D_i,\tau)$ is not consistent with the initial equation $\zeta(D,\tau)$).

Parker and Klingeman [1982] developed a fractional equation they fitted on the field data measured on the Oak Creek river [*Milhous*, 1973]. To go even further in adapting the model to the field reality, they used the bed grain size distribution. However, they used the sub-surface grain size distribution, much closer to the bedload grain size distribution than the much coarser bed surface grain size distribution. This control of subsurface sediment by the coarse surface layer, as well as exchanges with the bedload layer has been well described and theorized [*G. Parker and Klingeman*, 1982].

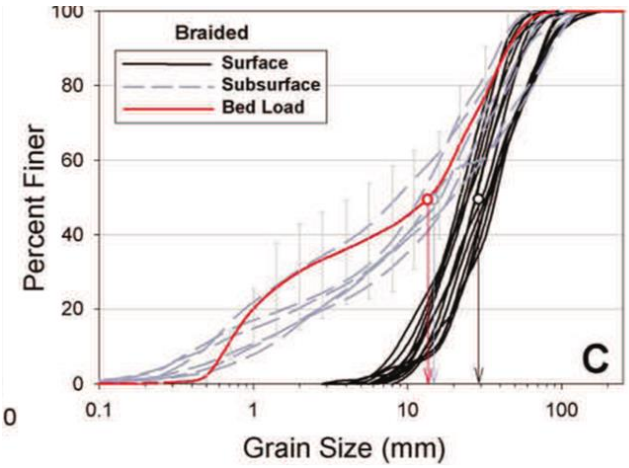


**Figure 19: Comparison between surface, subsurface and bedload grain size distribution [*Mueller and Pitlick*, 2014]**

### 6.1.6 Surface based calculation

Even if the observation that the bedload grain size distribution is in general very close to the subsurface grain size distribution (and very different from the surface grain size distribution) has been verified many times, the use of the subsurface grain size distribution is challenging in practice because this data is very complicated to collect and is generally not available. On the other hand, the surface grain size distribution is really easy to collect (e.g. by Wolman visual method).

This motivated Parker [1990] to adapt his equation and propose a 'surface based approach' i.e. computation with the surface grain size distribution. Following the same idea, Wilcock et al. [2001] performed a series of flume experiments with non-uniform materials, to construct a unique dataset where each solid discharge is systematically associated with the associated bed surface composition. Wilcock and Crowe [2003] then used this data set to construct a surface based equation that is widely used today.

This surface based approach is also true when a model is built with field data [*Recking*, 2010], because bedload values are systematically associated with the bed surface grain size distribution; the question can then be reduced to a purely mechanical problem (without any consideration for equilibrium concept):

- For a given material in place (the bed)
- and a force exerted on this material (the bed shear stress)
- what will move (in quality and quantity)?

But if the bed subsurface contributes to bedload, it also means that we conceptually use the mobility of the coarse surface as a proxy for the availability of subsurface materials, according to

the armor mobility process described by Parker and Klingeman [1982]. This process is considered to remain valid during flood conditions, the armor layer being mobile but still in place [*Clayton and Pitlick*, 2007; *Peter R. Wilcock and DeTemple*, 2005], including during erosion and aggradation phases as shown in Figure 20.

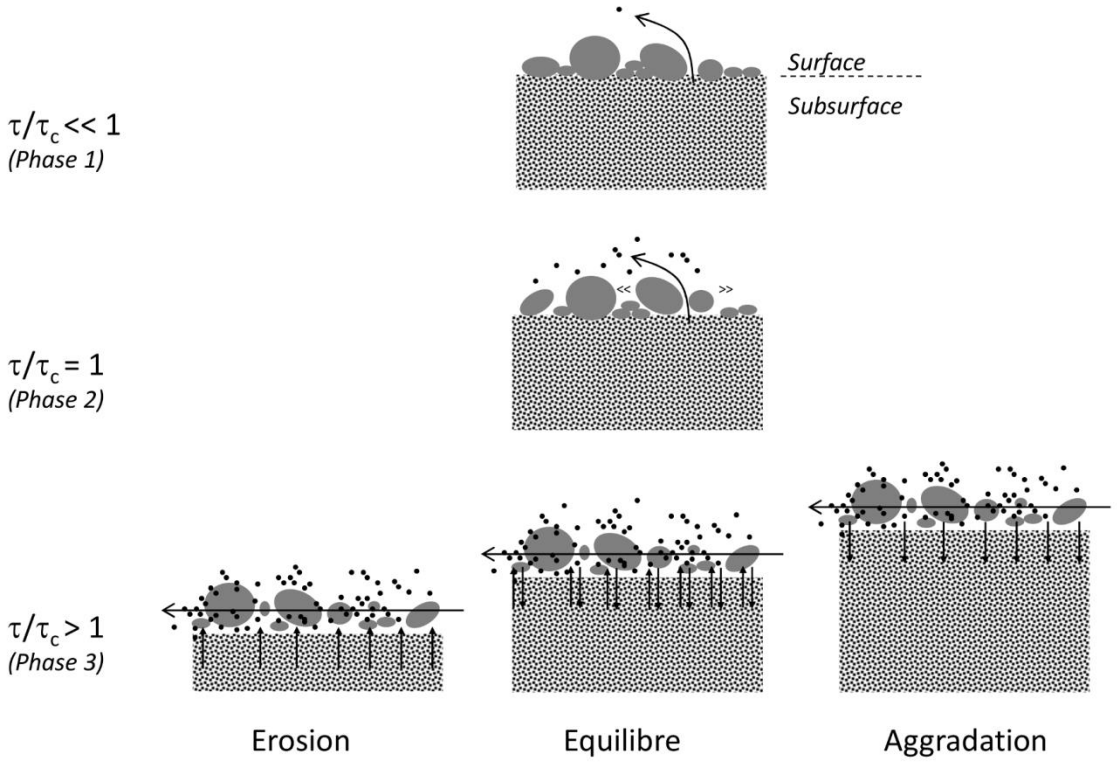


**Figure 20: Diagram presenting the conceptual approach where surface mobility serves as a proxy for the mobility of the bed as a whole, with a surface layer more or less mobile but still in place, and regulating exchanges with the subsurface**

It should be noted that this approach ignores the concept of equilibrium as it has been defined in the laboratory (constant slope and equality of inlet and outlet solid discharge). The notion of equilibrium does not completely disappear however: since the hydraulic force is calculated from the geometric properties (slope, section), a nonetheless essential condition is that the section is self-formed in its alluvium.

### 6.1.7 Section self-formed in its alluvium

In the best case, for a given section, an equation will relate the hydraulics generated by the bed material in place and the transport (of a part or all) of this same material.

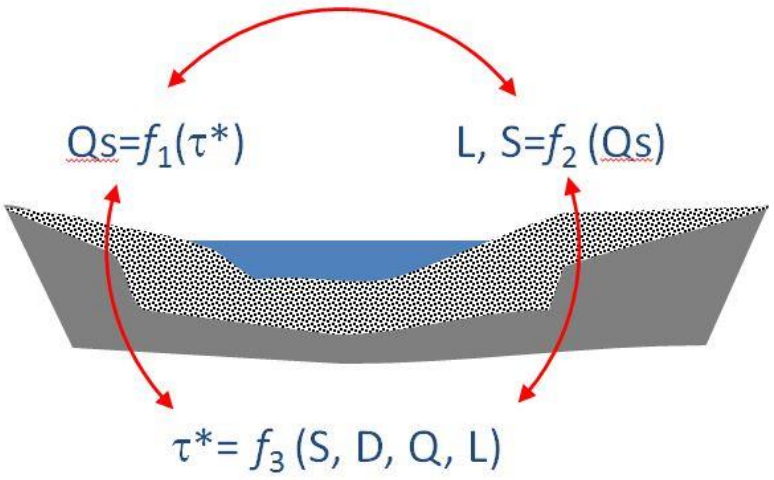


**Figure 21: Feedback principle between hydraulics, transport and geometry.**

For example, an equation will be unable to predict bedload if the transported sediments measured in the control section originates from an upstream reach where the prevailing hydraulics and sediments processes are very different than the conditions prevailing in the control section used for computation. It can be illustrated in the following example, where the downstream section (narrow bed, paved and steep slope because constrained laterally by the road) receives the sediment produced by the upstream braiding reach.

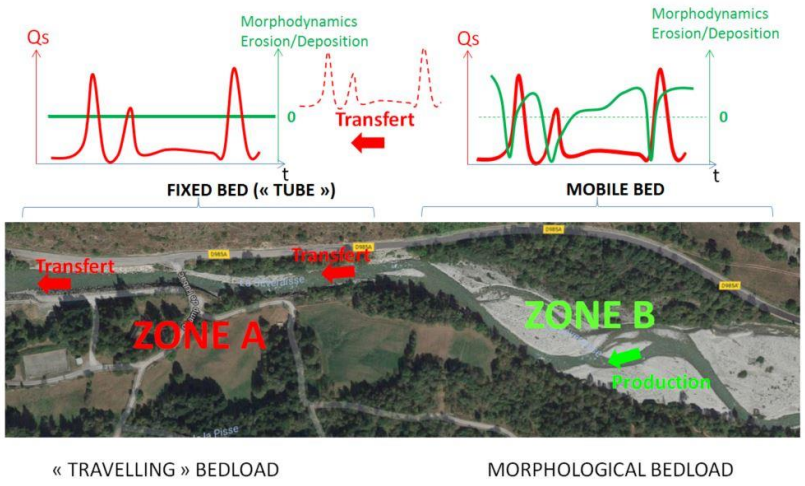


**Figure 22: Relationship between morphology and sediment transport**

In this example, we shown that the transport rates measured in the downstream reach are best reproduced with data collected in the upstream braiding reach[*Misset et al.*, 2020b].

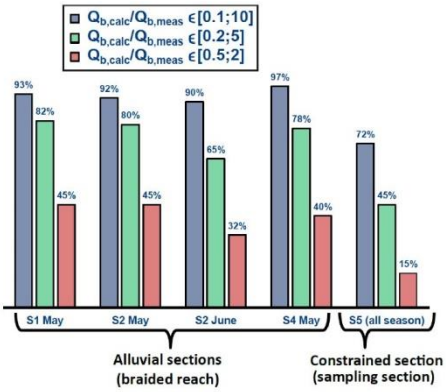


**Figure 23: Comparison of bedload measured and calculated in the Séveraisse River, with consideration of different sections for the input data [*Misset et al.*, 2020b]**

### 6.1.8 Travelling and morphological bedload

In the previous example sediments transiting in the downstream reach is disconnected from this reach production as it originates from upstream, and is called 'traveling bedload' [*Yu et al.*, 2009]. Bedload produced and transiting in the braiding reach is called morphological bedload as it a priori closely matches the local morphology changes.

Travelling bedload may not be negligible in mountain streams where rivers alternate alluvial zones with narrow, very stable and steep paved sections (because they transfer very efficiently downstream the incoming sediments with no or poor local interactions with the bed, these reaches are sometimes nicknamed 'tube' by analogy to what could be the transport in a steep concrete tube). Alluvial zones must be considered for the calculation, however they are sometimes absent (channel supplied directly by hillslope processes) or simply inaccessible. In this case the modeling remains complicated; however, tests have shown that the use of transport formulas with the grain size distribution of the transported materials (as it can be measured in local deposition zones) makes it possible to considerably improve the prediction of transported volumes [*Piton and Recking*, 2017]. It must be noted that, contrarily to computation of alluvial reaches, in this case the computation strategy requires 2 grain size distribution, as the bed grain size distribution is still required for computing the hydraulics.

It must be also noted that stable mountain streams, such as step-pools, can behave differently during their long term evolution: most of the time they are stable (with very coarse surface pavement) with low transport reduced to travelling bedload. But during large and rare floods, their morphology can be totally recomposed by destruction of the bed pavement. Several studies have shown that step-pool destructions are associated with large return periods (>20-50 yrs) [*Chin*, 1998; *G Grant et al.*, 1990; *Molnar et al.*, 2010; *Recking et al.*, 2012; *Whittaker and Jaeggi*, 1982] and can be followed by a long recovery period with the sediment being supplied from the disturbed bed [*Lenzi*, 2001; *Lenzi et al.*, 2004; *Turowski et al.*, 2009].

### 6.1.9 Variability

What characterizes the most rivers and their functioning is a very strong spatial and temporal variability. Spatial variability concerns all the data needed for calculations, such as grain size distribution or channel depth in a given section. Bedload transport variability is observed in almost all measurements, as shown in Figure 24.

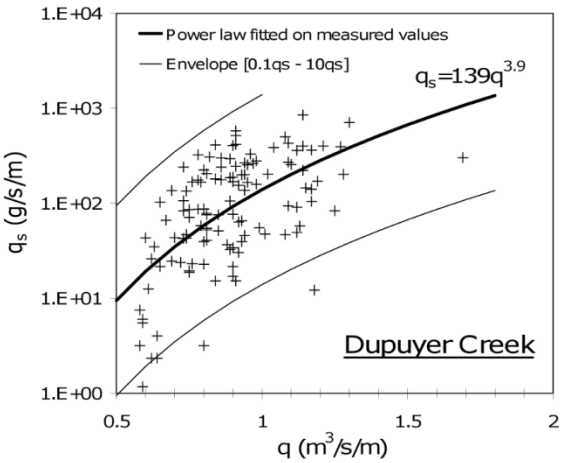


**Figure 24: Bedload variability in Dupuyer Creek [*A C Whitaker and D Potts*, 2007]**

It can be seen in Figure 24 that to a given unit flow discharge $q$ corresponds a wide range of solid discharge values $q_s$ covering two orders of magnitude. This scatter is common to almost all datasets (viewable on BedoadWeb). It can partly be explained by measurement uncertainties, but this is far to be the only reason: this range of fluctuation is inherent to the transport process itself and bedload variability is also measured in perfectly controlled flume conditions [*Ancey*, 2019b]. Among the physical causes we can mention turbulence, bedforms (dunes ...), grain sorting [*Bacchi et al.*, 2014], and seasonality.

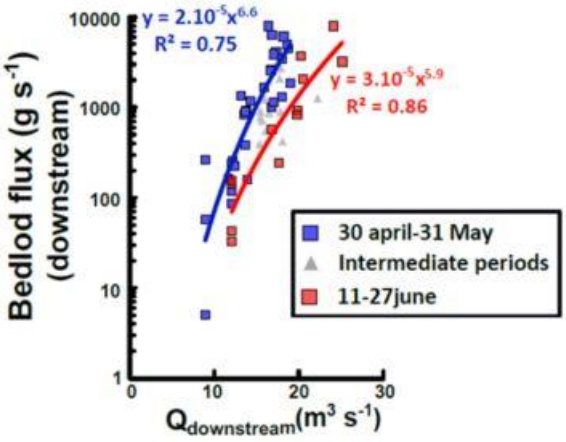


**Figure 25: Seasonal bedload variability in the Séveraisse River [*Misset et al.*, 2020a]**

The seasonality effect is shown in **Figure 25**, and is related to the different possible states of the bed (sediment recharge and paving more or less pronounced) at different times of the year. This variability can a priori be anticipated with input data for calculation collected for each season.

What must be concluded from this section on variability is that a transport equation can best reproduce a median trend (**Figure 24**). Probabilistic approaches would be more appropriate to take into account the extent of the phenomenon [*Ancey*, 2019a] and thus give, for a given flow condition, not a single bedload transport value, but a median and the distribution around this median.

### 6.1.10 Morphological or local equations ?

The high variability of data used to calculate bedload transport complicates the use of flume derived equations for field applications. Indeed, because of the strong non-linearity of bedload response to shear stress (a very small shear stress variation can lead to very strong flux differences, especially close to the beginning of movement), the computation with an average depth applied to the whole section can considerably underestimate the transport rate that would exist locally under a high water level, for this same average water level [*Recking*, 2013b].

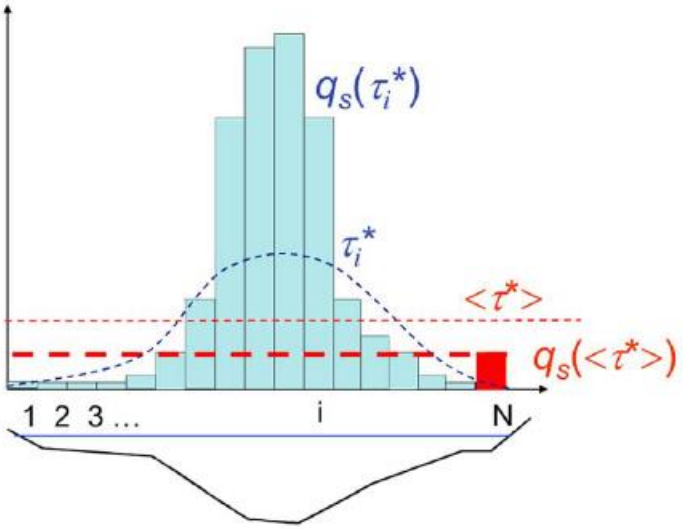


**Figure 26: Effects of variability over the section : results of calculation with an average water depth ($q_s(<\tau^*>)$, in red) will be lower than the sum of local calculations ($\sum q_s(\tau_i^*)$ in blue) [*Recking*, 2013b]**

Equations constructed with field data partially overcome this problem because in the data sets used, the measured transport values are associated with hydraulic quantities averaged over the section (and therefore implicitly taking into account this variability). These 'morphological equations' are thus constructed for a 1D calculation with 1D data (variations in topography or grain size will be taken into account only in the flow direction). Because the variability on the

section changes with the morphology, these equations should logically be adapted according to the local bed morphology [*Recking et al.*, 2016]

On the other hand, equations derived from narrow flume experiments are constructed to reproduce a (univocal) relation between shear stress and local flow, and do not have in their DNA any morphological signature, which must by consequence be taken into account elsewhere (for example via a 2D modeling of hydraulics and sediment transport).

### 6.1.11 Width and active width

Most bedload equations give access to a unit transport $q_s$[m$^3$/s/m], which must then be multiplied by a width to access the total transport: the active width $W_a$. From a hydraulic point of view, the flow width $W$ is available, so that $W_a \leq W$:

$$Qs = W_a q_s \quad \text{with} \quad W_a \leq W \tag{46}$$

The definition of active width is not always trivial and depends on the person doing the study. It is therefore a subjective and delicate criterion because it will directly impact the result of the calculation.

**Figure 27: Active width (in red) to be distinguished from the total width**

The maximum active width is delimited by the part of the bed (including the water zone and emerged lateral bars) potentially mobilized by the flow during floods. It can be straightforward and confused with the minor bed in constrained river reaches. The definition is more delicate for large alluvial valley, and especially for a braiding rivers where the morphodynamically active width can be very large and so the risk to overestimate the active width (and thus bedload computation) is strong.

Actually the main channel developed in a large alluvial plain is not characteristics of a single flood, but results from a succession of floods, and thus its cross section could be considered representative for the maximum envelop for the active width to be considered for most common transports events (the bankfull geometry is usually considered to be representative for a 2-5yrs return period). The question is more delicate for exceptional floods for which two hypothesis are possible:

1) enlargement of the main channel and of the active width
2) the maximum active width is still limited to the main channel and water in excess is transferred to the flood plain with no transport effects.

Part of the response can be found the literature concerning breading rivers, where available observation suggests that even in large flood, the transporting zone seems limited to the low flow main channel geometry which migrates and sweeps the braiding area.

**Figure 28: Active width (in red) in a braiding section. We make the hypothesis that during large floods the active width is limited to a main channel which migrates and sweeps the alluvial plain.**

# 6.2 Bedload equations

Before starting this part, it should be noted that there are dozens of transport equations in the literature, and that only a few of them have been implemented so far in BedloadWeb and are presented in the following. It is not excluded in the future to add new equations to the website.

Several papers have traced back the story of these formulas and bring full details on their genesis [*Ancey*, 2019a; *Hager*, 2005; *Gary Parker*, 2009]. We will just recall here the equations and as far as possible their limits (for more details see the original papers).

### 6.2.1 Bagnold [1980]

***Formulation***

$$q_b[m^3/m/s] = \frac{q_{v*}}{\rho_s - \rho}\left[\frac{\omega - \omega_c}{(\omega - \omega_c)*}\right]^{3/2}\left(\frac{d}{d*}\right)^{-2/3}\left(\frac{D_m}{D*}\right)^{-0.5} \quad (47)$$

Where $d$ is the water depth, $\omega$ and $\omega_c$ are unit power and unit critical power:

$$\omega = \rho d S U = \rho q S \quad (48)$$

and

$$\omega_c = 290 D^{3/2} log\left(12\frac{d}{D}\right) \quad (49)$$

Bagnold omitted the gravity term $g$ in this definition of $\omega$. The asterisk (*) denotes the reference values used to adimensionalize each term. Bagnold proposed (from flume experiments with sands material) $q_v$*=0.1 kg/m/s, $^2(\omega - \omega_c)$*=0.5 kg/m/s, d*=0.1m and D*=0.0011 m.

***Note about thequation development***

Despite the reference values used to adimensionalize the formula were deduced from laboratory data with 1.1 mm sand [*Williams*, 1970], the formulation was proposed by the author for a wide range of rivers ranging from sands to rivers with coarse load (validation by the author on rivers with $D_{50}$> 300mm)..

The critical power $\omega_c$ is deduced from the hypothesis of a critical Shields number equal to 0.04. The author warns for bimodal distributions with two distinct grain sizes, for which $\omega_c$ could result from a geometric mean of the values calculated for each fraction (in BedloadWeb this parameter is calculated by default with Eq.49, but users can change this value).

### 6.2.2 Camenen et Larson [2005]

***Formulation***

$$\Phi = 12\tau^{*3/2}\exp(-4.5\tau_c^*/\tau^*) \quad (50)$$

with

$$\tau_c^* = \frac{0.3}{1+1.2D*} + 0.055[1-\exp(-0.02D*)] \quad (51)$$

and

$$D^* = \left[\frac{(s-1)gD_{50}^3}{\nu^2}\right]^{1/3} \quad (52)$$

***Note about the equation development***

Formula initially developed for coastal transport, based on laboratory data (including Meyer-Peter Muller, Smart and Jaeggi, Gilbert, Brownlie, Nnadi & Wilson ... ) with diameters of 0.1 <*D* <200mm (essentially comprising sands) and relative density 1.14 <s <2.7.

### 6.2.3 Einstein-Brown [1950]

***Formulation***

$$\Phi = \left[\sqrt{\frac{2}{3}+\frac{36\nu^2}{g(s-1)D^3}} - \sqrt{\frac{36\nu^2}{g(s-1)D^3}}\right] f(\tau^*) \quad (53)$$

with

$$f(\tau^*) = 2.15\exp\left(-\frac{0.391}{\tau^*}\right) si\ \tau^* < 0.18 \quad (54)$$

$$f(\tau^*) = 40\tau^{*3}\ si\ \tau^* > 0.18 \quad (55)$$

***Note about the equation development***

This equation is a simplified version of the probabilistic formulation initially proposed by Einstein [1950]. Calibration was based on laboratory data from [*Gilbert*, 1914] and [*Meyer-Peter and Mueller*, 1948].

### 6.2.4 Engelund & Hansen [1967]

***Formulation***

$$\Phi = \frac{0.1}{f}\tau^{*5/2} \quad (56)$$

with

$$f = 2\frac{gRS}{U^2} \quad (57)$$

***Note about the equation development***

This equation has been established for transport over sand dunes:
- The theoretical framework considers an energetic balance for the transfer of sand over the dune height
- The exponent 2.5 applied to $\tau^*$ comes from an approximation valid for $\tau^*$> 0.15 (which is very large and valid for sands).
- The coefficient 0.1 comes from calibration with laboratory data [*Guy et al.*, 1966] (sand diameter of 0.19 - 0.93mm, 2.4m wide flume, slope 0.0004 <*S* <0.02).

### 6.2.5 Meyer-Peter & Muller [1948]

***Formulation***

$$\Phi = 8\left[\left(\frac{n'}{n}\right)^{3/2}\tau^* - 0.047\right]^{3/2} \quad (58)$$

The term *n*'/*n* is used for correcting the shear stress (for computing the grain shear stress as explained in §4.6).

***Note about the equation development***

Laboratory experiments with uniform and non-uniform materials.

Channel width: 0.35-2m, Slope: 0.0004-0.02 m/m, $D_{50}$: 0.4-29mm, $D_{84}$: 1.68-34.5mm, Water depth: 0.1-1.2m, Sediment density: 2.5-3.2kg/m3.

About field application, the authors specify : « *the test comprise a big region, namely from the beginning of bedload transport up to the big transport capacities of rolling bedload occurring in nature in streams in full flood…. The only assumption remaining is the requirement of good agreement between the particle composition of the moving bedload and that of the bed, i.e. the movability of the bed as occurring in nature in alluvial stretches*".

### 6.2.6 Parker [1979]

***Formulation***

$$\Phi = 11.2\frac{(\tau^* - 0.03)^{4.5}}{\tau^{*3}} \tag{59}$$

***Note about the equation development***

This formulation was calibrated on laboratory and field data [*Peterson and Howells*, 1973], obtained a priori for very fine materials (<1mm) (in [*Leo C. Van Rijn*, 1984]).

### 6.2.7 Parker [1990]

***Formulation***

This equation should be used with the grain size curve after removal of the sand fraction.

$$W_i^* = \frac{(s-1)gq_{vi}}{F_i u_{*s}^3} = 0.00218G(\phi) \tag{60}$$

with

$$\phi = \omega\phi_{sgo}\left(\frac{D_i}{D_g}\right)^{-0.0951}, \quad \phi_{sgo} = \frac{\tau_g^*}{\tau_{ssrg}^*}, \quad \tau_g^* = \frac{\tau}{\rho(s-1)gD_g}, \quad \tau_{ssrg}^* = 0.0386$$

$$G(\phi) = \begin{cases} 5474\left(1 - \dfrac{0.853}{\phi}\right)^{4.5} \; pour\; \phi > 1.59 \\ \exp[14.2(\phi - 1) - 9.28(\phi - 1)^2] \; pour\; 1 \le \phi \le 1.59 \\ \phi^{14.2} \; pour\; \phi < 1 \end{cases} \tag{61}$$

$$\omega = 1 + \frac{\sigma}{\sigma_0(\phi_{sgo})}\left[\omega_0(\phi_{sgo}) - 1\right]$$

Values of $\sigma_0(\phi_{sgo})$ and $\omega_0(\phi_{sgo})$ are read on the fllowing figure :

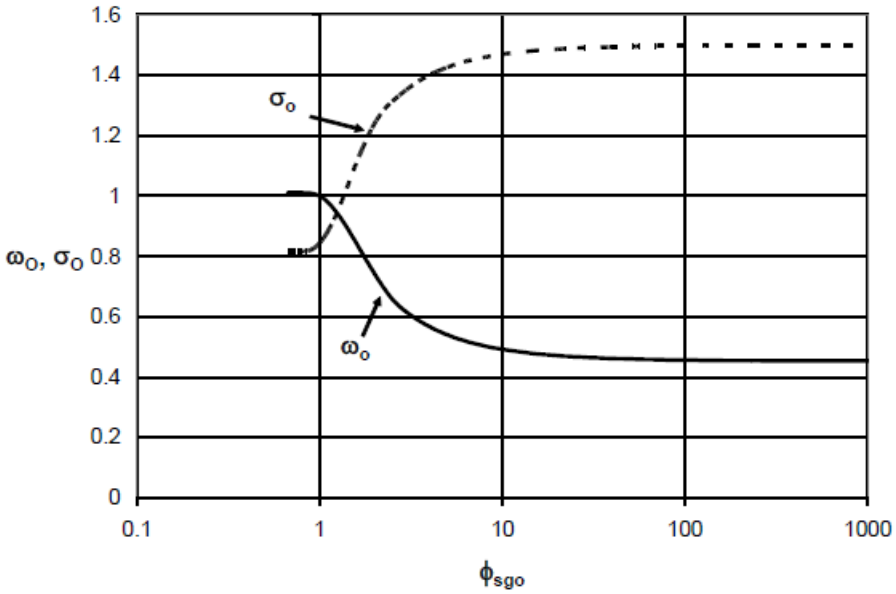


$D_g$ is the greometric grain size. The grain size distribution is divided into several classes i and we calculate :

$$\psi_i = \ln(D_i)/\ln(2), \quad \overline{\psi}_i = \frac{1}{2}(\psi_i + \psi_{i+1}), \quad p_i = p_f(\psi_{i+1}) - p_f(\psi_i) \text{ with } \sum p_i = 1$$

$$D_g = 2^{\psi_m} \text{ with } \quad \psi_m = \sum_{i=1}^{n} \overline{\psi}_i p_i,$$

$$\sigma^2 = \sum_{i=1}^{n} \left(\overline{\psi_i} - \psi_m\right)^2 p_i$$

***Note about the equation development***

The equation was built to reproduce coarse bedload transport only (without sands), using the field data collected in the Oak Creek River [*Milhous*, 1973] : Slope $S$ =0.8-2%, $D_{50}$=54mm, $D_{84}$=80mm, $\tau^*/\tau_c^*$=0.11-1.04 (computed for $D_{84}$).

### 6.2.8 Recking [2013a]

The model is shown schematically in the following figure, where the parameter $\tau_m^*$ is a mobility Shields stress delimiting partial transport ($\tau^* < \tau_m^*$) from total transport ($\tau^* > \tau_m^*$). The value of $\tau_m^*$ gives its shape to the model. It depends on several factors such as slope, grain size distribution, morphology. It can be calibrated or calculated.

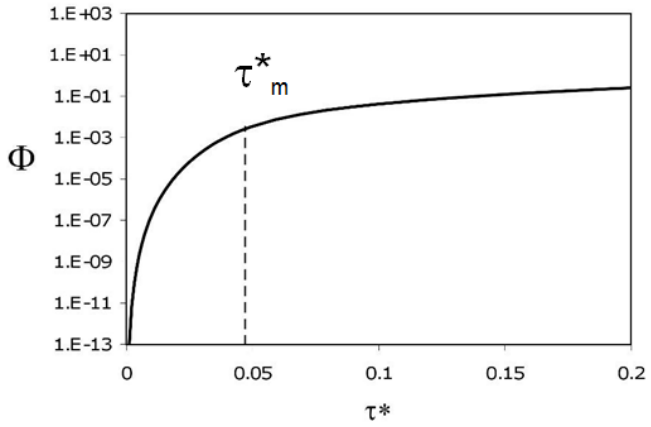


***Formulation***

Two versions of the model exist: a version for the field and a version for the lab (and for 2D modeling).

- **Version for the field, to be used with quantities (τ, slope, granulo, width ....) averaged over the section and at the reach scale:**

A first formulation written in two equations [*Recking*, 2010] was then reduced to a single equation [*Recking*, 2013a] :

$$\Phi = 14\frac{\tau^{*2.5}}{1+\left(\frac{\tau_m^*}{\tau^*}\right)^4} \quad (62)$$

Where Φ and τ* are calculated for diameter $D_{84}$, and where $\tau_m$* can be estimated with [*Recking et al.*, 2016]:

For riffle-pools and alternate bars $\tau_m^* = (5S + 0.06)\left(\frac{D_{84}}{D_{50}}\right)^{4.4\sqrt{S}-1.5}$ (63)

For other morphologies $\tau_m^* = 1.5S^{0.75}$ (64)

(For sand bed rivers, $\tau_m$* doesn't matter because flows generally check $\tau^* >> \tau_m^*$)

*!! It means that in BedloadWeb the choice of morphology associated with the section can therefore impact the result for this bedload equation !!*

The Shields number τ* can be calculated from the flow depth or hydraulic radius (Eq. 5) and $D_{84}$. But when only discharge is available it can also be estimated simply with the following equation (combination of Eq.5 et 24):

$$\tau^* = \tau_{D_{84}}^* = 0.015\frac{S}{s-1}\frac{q^{*2p}}{p^{2.5}} \quad (65)$$

where $q^* = \frac{q}{\sqrt{gSD_{84}^3}}$ is a dimensionless solid discharge [*Rickenmann and Recking*, 2011] and p=0.23 when q*<100, and p=0.31 otherwise.

- **Version for the lab or for local 2D calculation, to be used with local data (2D data averaged on the vertical)**

The previous formulation was calibrated on field data averaged at the reach scale and implicitly taking into account variability associated with the local morphology. This variability necessarily introduces a bias when the equation is considered for local transport (1D in the flume or on a flow vertical) [*Recking*, 2013b]. This is why a variant has been calibrated only on laboratory data [*Recking et al.*, 2016] :

$$\Phi = 14\frac{\tau^{*2.5}}{1+\left(\frac{\tau_m^*}{\tau^*}\right)^{10}} \quad (66)$$

with

$$\tau_m^* = 0.26S^{0.3} \quad (67)$$

As the flume data were obtained with almost uniform sediment mixtures, it is still unclear which characteristic diameter should be used in the field for Φ and τ* ($D_{50}$, $D_m$, $D_{84}$?). This validation is still necessary (for example by comparing a 2D computation with measured solid discharge).

***Note about the equation development***

From flume and field data (Tableau 2):

- The part of the model verifying $\tau^* < \tau_m^*$ was calibrated with the field data only.
- The part of the model verifying $\tau^* > \tau_m^*$ was calibrated with the flume data (in the absence of field data for this transport range).

Only 1/3 of the field data set was used to build the model. The remaining 2/3 were used for validation.

### 6.2.9 Rickenmann [1991]

***Formulation***

$$q_v[m^3/s/m] = 1.5(q - q_c)S^{1.5} \quad \text{for } 0.0004<S<0.2 \tag{68}$$

$$q_v[m^3/s/m] = \frac{12.6}{(s-1)^{1.6}}\left(\frac{D_{90}}{D_{30}}\right)^{0.2}(q - q_c)S^2 \quad \text{for } 0.03<S<0.2 \tag{69}$$

with

$$q_c = 0.065(s-1)^{1.67} g^{0.5} D_{50}^{1.5} S^{-1.12} \tag{70}$$

and $(D_{90}/D_{30})^{0.2}$=1.05 when unknown.

***Note about the equation development***

Flume data from Meyer-Peter & Muller, Smart & Jaeggi and new experiments to study the effect of water density on transport efficiency.

### 6.2.10 Schoklitsch [1962]

***Formulation***

$$q_v[m^3/s/m] = \frac{2.5}{\frac{\rho_s}{\rho}} S^{\frac{3}{2}}(q - q_c) \tag{71}$$

with

$$q_c = 0.26(s-1)^{5/3}\frac{D_{40}^{3/2}}{S^{7/6}} \tag{72}$$

***Note about the equation development***

Chanson [1999] states that the formulation was obtained from laboratory data (Gilbert) and field data (Danube and Aare). The equation should be used with the subsurface $D_{40}$ after [*J. C. Bathurst*, 2007]. However, because this data is never available the surface $D_{50}$ is used.

### 6.2.11 Smart & Jaeggi [1983]

***Formulation***

$$\Phi = 4\left(\frac{D_{90}}{D_{30}}\right)^{0.2} S^{0.6}\frac{U}{u^*}\tau^{*0.5}(\tau^* - \tau_c^*) \tag{73}$$

with

$$\frac{U}{u^*} = 2.5\left[1 - \exp\left(-\frac{0.05Z_{90}}{S^{0.5}}\right)\right]^{0.5} \ln(8.2Z_{90}) \quad (74)$$

$$\tau_c^*(S) = 0.05\cos(\text{arctg}(S))\left(1 - \frac{S}{tan\phi}\right) \quad (75)$$

Where $Z_{90}=R/D_{90}$ and $\phi=35°$ (0.61rd).

***Note about the equation development***

With flume data from Meyer Peter Muller plus new experiments with uniform and non-uniform materials: Channel width: 0.2m, Channel length: 6m, Slope: 0.03-0.25 m/m, $D_{50}$: 2-10.5mm, $D_{84}$: 2.4 -12.6 mm, water depth: 0.01-0.09 m, moving bed (no armor).

Not recommended by the authors for $D_{90}/D_{30}$> 8.5 and for slope $S$> 20%

### 6.2.12 Van Rijn [1984]

***Formulation***

$$\Phi = 0.053\frac{T^{2.1}}{D_*^{0.3}} \quad (76)$$

with

$$D_* = D_{50}\left[\frac{(s-1)g}{\nu^2}\right]^{1/3}, \quad T = \frac{u_*^2 - u_{c*}^2}{u_{c*}^2}, \quad (77)$$

$$u_* = \sqrt{g}\frac{U}{18\log(\frac{4R}{D_{90}})}, \qquad u_{c*}^2 = g(s-1)D_{50}(\alpha D_*^{\beta}) \quad (78)$$

Coefficients α and β are given in the following table:

| $D_*$ | α | β |
|---|---|---|
| $D_*$<4 | 0.24 | -1 |
| 4 < $D_*$ < 10 | 0.14 | -0.64 |
| 10 < $D_*$ < 20 | 0.04 | -0.10 |
| 20 < $D_*$ < 150 | 0.013 | 0.29 |
| 150 < $D_*$ | 0.055 | 0 |

***Note about the equation development***

Equation established for the transport of sand.

Calibration with flume data, validation with flume and field data.

### 6.2.13 Wilcock and Crowe [2003]

***Formulation***

$$W_i^* = \begin{cases} 0.002\phi^{7.5} & si\ \phi < 1.35 \\ 14\left(1 - \frac{0.894}{\phi^{0.5}}\right)^{4.5} & si\ \phi \geq 1.35 \end{cases} \quad (79)$$

with

$$W_i^* = \frac{(s-1)gq_{vi}}{f_i u_*^3}, \qquad \phi = \frac{\tau}{\tau_{ri}} \quad , \qquad \tau_{ri} = \tau_{rg}\left(\frac{D_i}{D_g}\right)^b \quad , \qquad b = \frac{0.67}{1+exp\left(1.5-\frac{D_i}{D_g}\right)} \quad (80)$$

$$\tau_{rg} = (s-1)\rho g D_g(0.021 + 0.015exp[-20F_s])$$

Where $q_{vi}$ is the volumetric transport per unit width and for grain size i ($q_b = \Sigma q_{vi}$), $D_g$ is the bed surface geometric mean diameter (see Parker 90), $F_s$ is the fraction of sand on the bed surface ($F_s \leq 1$).

The following formulation was proposed for correcting the shear stress for bedform resistance, when required [*P Wilcock et al.*, 2009]:

$$\tau' = 17(SD_{65})^{1/4}U^{3/2} \quad (81)$$

where $D_{65}$ must be given in mm.

***Note about the equation development***

This formula was constructed from flume data with non-uniform grain size distribution (sand and gravel mixtures) on slopes varying from 0.1 to 1.8%. A particularity, compared to the other flume derived equations, is that each individual solid discharges value was not associated to the grain size distribution of the injected material but to the grain size distribution the bed surface at the time of the measurement ('surface based approach') what makes it more legitimate for use in the field.

### 6.2.14 Wong & Parker [2006]

***Formulation***

$$\Phi = 3.97[\tau^* - 0.0495]^{3/2} \quad (82)$$

***Note about the equation development***

Re-analysis of Meyer-Peter & Muller data

# 7 BEDLOAD GRAIN SIZE DISTRIBUTION

## 7.1 Fractional calculation

Some transport equations permit a fractional calculation which consists of calculating a solid discharge $q_{si}$ for each grain size class i present on the river bed. Knowing the total solid discharge $q_s$, and solid discharges $q_{si}$ associated with each diameter $D_i$ present at the bed surface, it is easy to calculate the transported fraction $q_{si}/q_s$ corresponding to each class $i$ and to construct the corresponding bedload grain size distribution. In BedloadWeb it concerns the Parker [*G. Parker*, 1990] and Wilcock and Crowe [*P.R. Wilcock and Crowe*, 2003] equations.

## 7.2 Modelling the bedlload GSD

However most transport equations give an estimate of the bulk (total) transport $q_s$, and do not give access to the corresponding grain size distribution. This is why the GTM (Greneralized Threshold Model) method has been proposed and allows a computation totally independent of bedload transport calculation. This method extends the concept of threshold transport to each particle size class; it is presented in detail in an article [*Recking*, 2016], and a simple summary is proposed here.

GTM consider that we know a critical Shields stress $\tau_{cRef}$* for a given reference diameter $D_{\text{ref}}$ and that the hiding function (Eq.35) can be written:

$$\tau_{ci}^{*} = \tau_{cRef}^{*} \left( \frac{D_i}{D_{Ref}} \right)^{\alpha} \tag{83}$$

BedloadWeb considers by default Ref=84 with [*Recking*, 2009]:

$$\tau_{cD84}^{*} = \frac{\tau}{g(\rho_s - \rho)D_{84}} = 0.56S + 0.021 \tag{84}$$

But it is possible to change both $D_{Ref}$ and the corresponding $\tau_{cRef}$*.

- *Competent flow*

The flow competence method [Andrews, 1983; Carling, 1983] considers that for a given bed grain size distribution (comprising diameters between $D_1$ and $D_{100}$), at a given flow characterized by a Shields stress $\tau$* will be associated a maximum transported diameter of size $D_M$ (with $D_1 \leq D_M \leq D_{100}$). The corresponding M percentile must be determined.

Rearranging Eq.83 and postulating that the proportionality between diameters also holds for the grain size distribution percentiles, we obtain:

$$\mathrm{M} = \mathrm{Ref}\left(\frac{\tau^*}{\tau_c^*}\right)^{\beta} \tag{85}$$

Where M ∈[1-100] is the particle size index (in reference to the bed grain size distribution) characterizing the maximum transported diameter $D_M$, and where $\tau^*$ and $\tau_c^*$ are computed for $D_{Ref}$, and where $\beta$>0 is a coefficient such that:

- $\beta$ <1 simulates a sandy bed with nonzero transport when $\tau^*/\tau_c^*$ is vanishingly small.
- $\beta$ =1 simulates linear dependence between grain size $D_M$ and shear stress
- $\beta$ >1 simulates non-linear dependence; in particular, a high value ($\beta$ >10) simulates near-equal mobility in a paved bed.

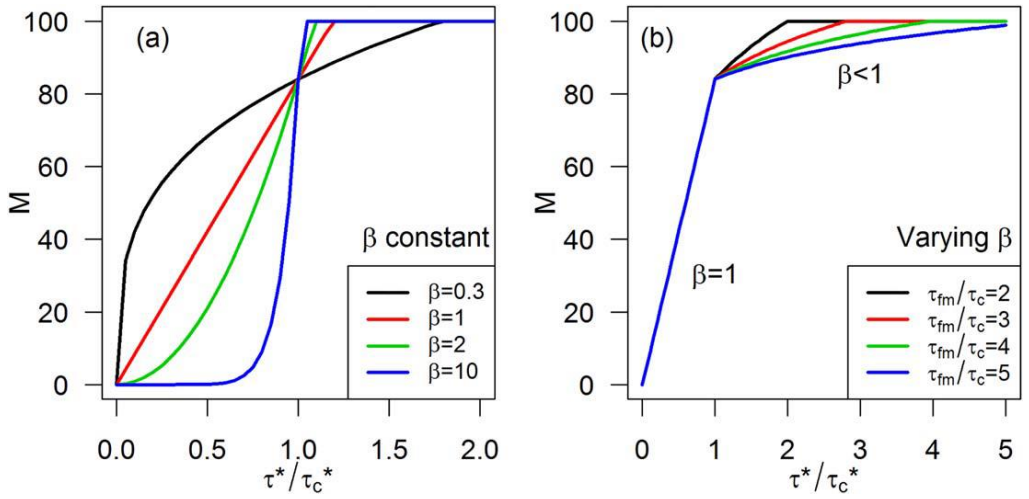


**Figure 29: Variation of the maximum transported size index M with $\tau^*/\tau_c^*$, for Ref=84, (a) for constant β values and (b) distinguishing the low (β=1 in the example) and high transport conditions**

To avoid an abrupt transition when $\tau^*/\tau_c^*$>1, the $\beta$ coefficient was modeled with (see Recking 2016 for more details):

$$\beta_{\tau^*/\tau_c^*>1} = \frac{13.4 - 2.91\ln(Ref)}{\tau_{fm}^*/\tau_c^*} \tag{86}$$

where $\tau_{fm}$ designates the shear stress threshold for full mobility of the whole bed mixture (comprising $D_M$). In BedloadWeb $\tau_{fm}/\tau_c$=2 by default (but the user can change this value).

- *Partial or full mobility*

Once the maximum size $D_M$ of the bedload material is defined, it is assumed that all sizes smaller than $D_M$ and present at the bed surface are also in motion.

However for a given class i in motion ($D_i < D_M$), how to define its mobility? The concept of partial transport considers that only a part of this class of grains is in motion, the rest being at rest [*P.R. Wilcock and Mc Ardell*, 1997]. Conversely, a given class could be considered fully mobile as soon as it is mobilized by the flow. The current state of knowledge does not allow to decide, and probably the mobility may depend on the morphology and degree of bed armoring.

GTM does not give answer to this question, but uses a function that simulates each situation. Thus the fraction $\varphi_i$ mobilized in each size class of bed surface will be given by:

$$\varphi_i = \varphi_0 + \left(1 - \left(\frac{i}{M}\right)^{\gamma}\right) \tag{87}$$

Where $\varphi_0$ is the fraction we consider minimum (default is 0.01), and where the exponent $\gamma$ imposes the maximum and decay rate of $\varphi_i$ when coarser and coarser bed materials are considered.

Figure 30 illustrates the behavior of Eq.87 for different $\gamma$ values:

- $\gamma$ weak implies that in a given size class the material is partially mobile.

- $\gamma$ strong implies full mobility of the size class as soon it is solicited by the flow

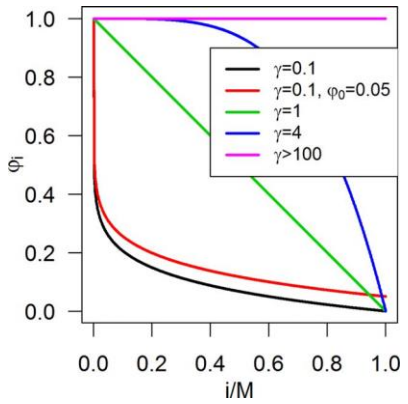


**Figure 30: Fraction $\varphi_i$ of the i[th] bed surface percentile (i[0,M]), which is mobile for the given shear stress.**

The choice of $\gamma$ is not obvious for the reasons recalled above, and it is even more complex if one considers that a priori there is no reason for $\gamma$ to be constant. It could evolve when the flow increases, with for a given class *i*, a partial transport at low flows which tends towards full mobility when the flow increases; for example small gravels could be partially mobile at low flows and become fully mobile at higher flows for which pebbles would still be in partial transport. This is why a new function has been proposed linking $\gamma$ to $\tau^*/\tau_c^*$:

$$\gamma = \gamma_0 + \gamma_1 \left(\frac{\tau^*}{\tau_c^*}\right)^{\gamma_2} \quad (88)$$

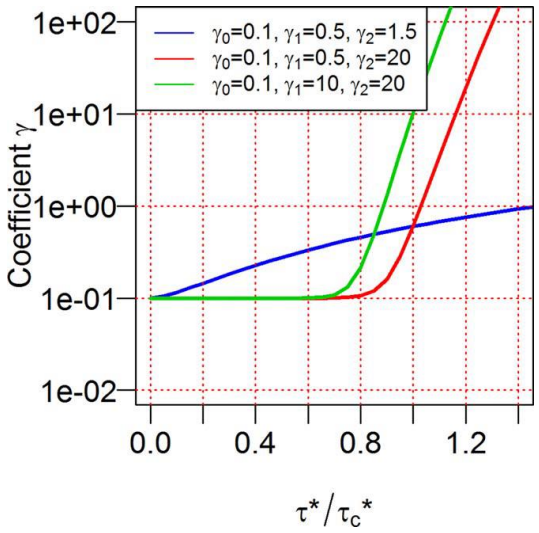


**Figure 31: Variation of the gamma coefficient (i.e., of sediment mobility in a given class) with the transport stage.**

The term $\gamma_0$ is 0.1 by default, and the terms $\gamma_1$ and $\gamma_2$ depend on the sediment mobility. Their definition is unfortunately, once again, challenged by our poor knowledge of the bed mobility in general. A calibration was done considering two different situations:

- The Wilcock and Crowe equation fitted on flume data with partial transport [*P.R. Wilcock and Crowe*, 2003]
- The field data from Oak Creek River, with a bed armor [*Milhous*, 1973]

Results are given in the following table and indicate that two distinct set of values were required for **β et $\gamma_2$**.

| | Wilcock and Crowe | Oak creek | Signification |
|---|---|---|---|
| $\beta\ (\tau/\tau_c>1)$ | 0.25 (computed) | 0.25 (computed) | Determine the maximum percentile *M* mobilized by the flow (Eq.85) |
| **$\beta\ (\tau/\tau_c<1)$** | **0.5** | **2** | |
| $\gamma_0$ | 0.1 | 0.1 | Determine the fraction $\varphi_i$ of a given percentile $i<M$, that is mobile for a given shear stress (Eq.88) |
| $\gamma_1$ | 0.5 | 0.5 | |
| **$\gamma_2$** | **1.5** | **20** | |
| $\varphi_0$ | 0.01 | 0.01 | Minimum value for $\varphi_i$ (Eq.87) |
| $\tau_{fm}/\tau_c$ | 2 | 2 | Determine the shear stress associated with M=100 |

**Tableau 3: Results of the GTM calibration obtained with the Wilcock and Crowe model and the Oak creek data**

All these coefficients can be modified in BedloadWeb. Working with Rhone river data, [*Vázquez-Tarrío et al.*, 2019] found good agreement using the Oak Creek calibration values. Validation work is still needed but it will only be possible new field data.

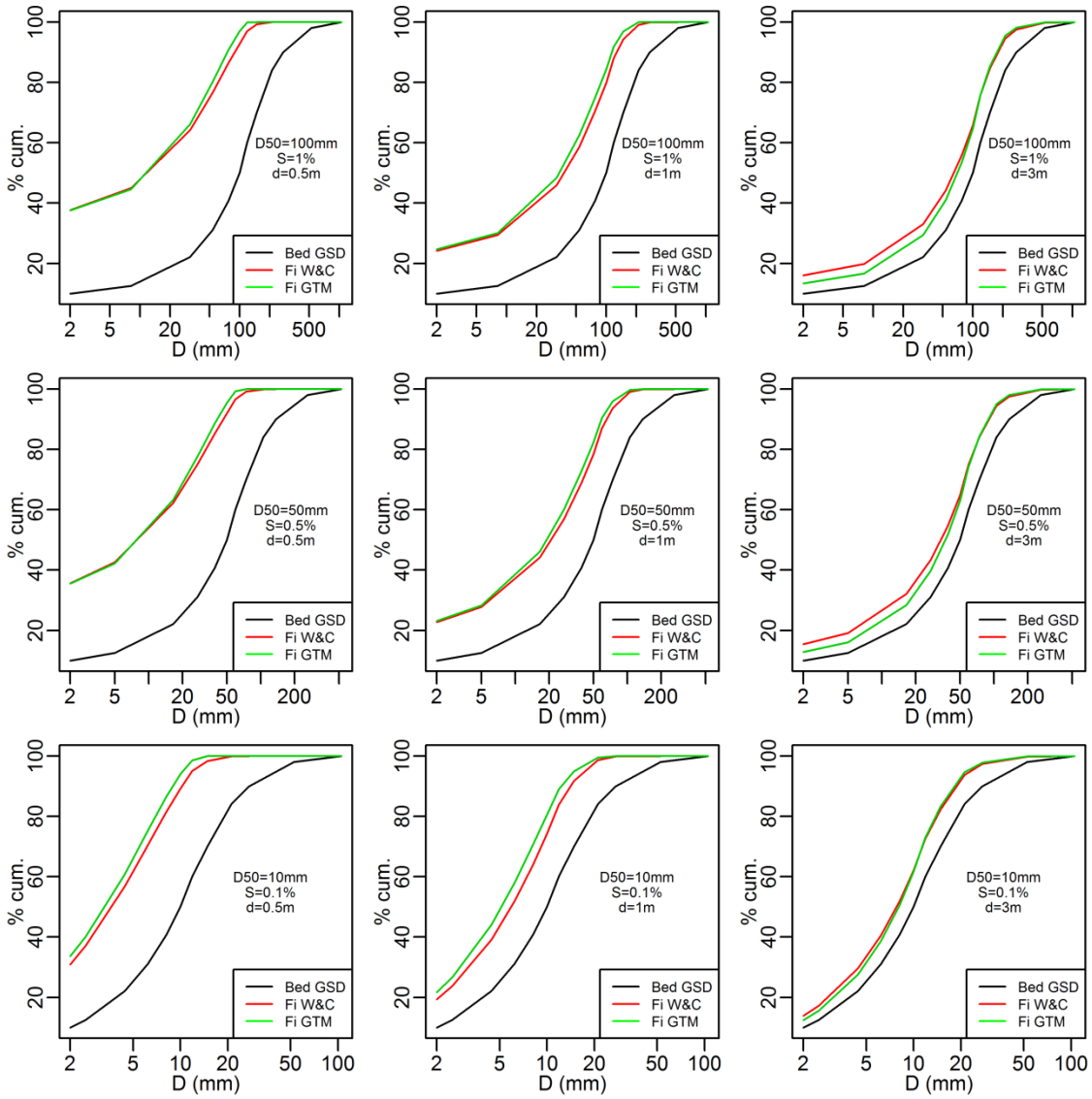


**Figure 32: Comparison between the Wilcock and Crowe equation and the GTM model for different transport conditions**

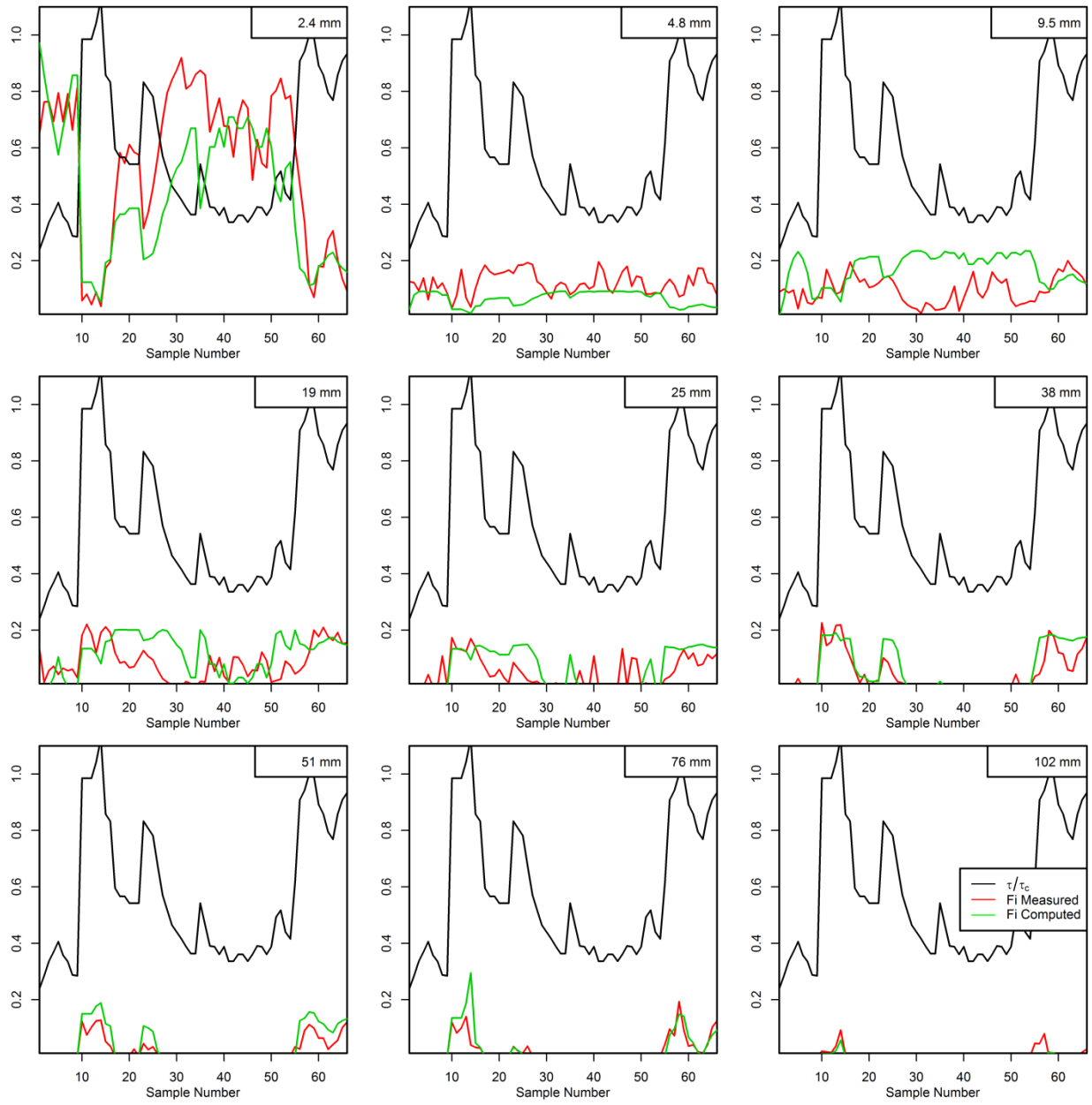


**Figure 33: Comparaison between the GTM model and the granulometry transported in Oak Creek**

# 8 CONCLUSION

All the concepts used in BedloadWeb have been recalled in this document, as well as the different equations. Sediment transport and fluvial morphology cannot be qualified as exact science, and this document reflects only the author's point of view. Not everything could be explained in detail, and some aspects may even feel imprecise. But the goal was to stay in a concise and easy-to-access format. It is not useless to recall, moreover, that for each aspect addressed in this manuscript, the reader will find an abundant literature on the net.

This document may be completed later.

# 9 APPENDIX

Summary of some flume experimental conditions

| Author | $D$ (mm) | $\sigma$ | $\rho_s$ (t/m$^3$) | Slope $So$ (%) | $W$ (m) | values | Observation |
|---|---|---|---|---|---|---|---|
| Cao 1985 | 22.2 | 1.29* | 2.57 | 1 to 9 | 0.6 | 124 | Steep slopes |
| | 44.3 | 1.21* | 2.75 | 1 to 9 | | | |
| | 11.5 | 1.24* | 2.65 | 0.5 to 1 | | | |
| Smart and Jaeggi 1983 | 4.3 | 8.46** | | 3 to 30 | 0.2 | 78 | Steep slopes |
| | 4.2 | 1.44** | | 5 to 20 | | | |
| | 2 | 4.6** | | 5 to 20 | | | |
| | 10.5 | 1.34** | | 3 to 20 | | | |
| Rickenmann 1990 | 10 | 1.34** | 2.68 | 7 to 20 | 0.2 | 46 | Bedload with various flow viscosities (clay suspension) |
| Meyer-Peter and Muller 1948 | 1.2 to 28.65 | | 1.25 to 4.2 | 0.3 to 1.7 | 0.35 à 2 | 133 | From Smart et Jaeggi (1983) |
| Bogardi and Yen 1939 | 10.34 | 1.18 | 2.63 | 1.2 to 2.5 | 0.83 | 44 | As reported by Brownlie (1981) |
| | 6.85 | 1.11 | 2.61 | 1 to 2.5 | 0.83 | | |
| | 15.19 | 1.11 | 2.64 | 1.1 to 2 | 0.3 | | |
| Casey 1935 | 1 | 1.16 | 2.65 | 0.1 to 0.5 | 0.4 | 90 | As reported by Brownlie (1981) |
| | 2.46 | 2.81 | 2.65 | | | | |
| Graf & Suszka 1987 | 12.2 | 1.52** | 2.72 | 0.75 to 1.25 | 0.6 | 114 | |
| | 23.5 | 1.53 | 2.74 | 1.5 to 2.5 | | | |
| Gilbert 1914 | 3.17 | 1.13 | 2.65 | 0.8 to 2 | 0.13 | 377 | As reported by Brownlie (1981) |
| | 4.94 | 1.13 | 2.65 | 0.6 to 3 | to | | |
| | 7 | 1.12 | 2.65 | 0.7 to 3 | 0.6 | | |
| | 0.506 | | | 0.3 to 2 | | | |
| HoPang-Yung 1939 | 1.4 | 1.96 | 2.64 | 0.1 to 0.5 | 0.4 | 80 | As reported by Brownlie (1981) |
| | 2.01 | 1.9 | 2.45 | | | | |
| | 3.13 | 2.24 | 2.49 | | | | |
| | 4.36 | 1.59 | 2.7 | | | | |
| | 6.28 | 1.49 | 2.66 | | | | |
| Mavis et al. 1937 | 4.18 | 1.23 | 2.66 | 0.1 to 1 | 0.82 | 283 | As reported by Brownlie (1981) |
| | 3.12 | 1.25 | 2.66 | | | | |
| | 2.03 | 1.29 | 2.66 | | | | |
| | 1.41 | 1.24 | 2.66 | | | | |
| | 3.73 | 1.30 | 2.66 | | | | |
| | 1.68 | 1.36 | 2.66 | | | | |
| Paintal 1971 | 22.2 | 1.07 | 2.65 | 0.1 to 1 | 0.91 | 81 | As reported by Brownlie (1981) |
| | 7.95 | 1.1 | 2.65 | | | | |
| | 2.5 | 1.08 | 2.65 | | | | |
| Julien and Raslan 1998 | 0.2 | 1.4** | 2.5 | 0.19 to 0.42 | 1.3 | 28 | High R/D, "sheet flow" |
| | 0.6 | 1.43 | 2.7 | 2.57 to 5.11 | | | |
| | 0.4 | 2.39 | 2.6 | 3 to 5.3 | | | |
| Einstein and Chien 1955 | 1.3 | 1.11 | 2.65 | 1.2 to 2.6 | 0.31 | 16 | As reported by Brownlie (1981), high R/D |
| | 0.94 | | | | | | |
| | 0.274 | | | | | | |
| Sumer et al. 1996 | 0.13 | | | 0.38 to 0.94 | 0.3 | 19 | High R/D, "sheet flow" |

# REFERENCES

Aberle, J., and G. M. Smart (2003), The influence of roughness structure on flow resistance on steep slopes, *Journal of Hydraulic Research*, *41*(3), 259-269.

Ancey, C. (2019a), Bedload transport: a walk between randomness and determinism 1. The State of the Art, *Journal of Hydraulic Research*, 1-24.

Ancey, C. (2019b), Bedload transport: a walk between randomness and determinism 2.Challenges and prospects., *Journal of Hydraulic Research*, 1-24.

Andrews, E. D. (1983), Entrainment of gravel from naturally sorted riverbed material, *Geological Society of America Bulletin*, *94*(10), 1225-1231.

Andrews, E. D., and G. Parker (1987), Formation of a coarse surface layer as the response to gravel mobility, in *Sediment transport in Gravel-bed rivers*, edited by J. W. sons, pp. 269-325.

Ashworth, P. J., and R. Ferguson (1989), Size-selective entrainment of bed load in gravel bed streams, *Water Resources Research*, *25*(4), 627-634.

Bacchi, V., A. Recking, N. Eckert, P. Frey, G. Piton, and M. Naaim (2014), The effects of kinematic sorting on sediment mobility on steep slope, *Earth Surface Processes and Landforms*, DOI: 10.1002/esp.3564.

Bagnold, R. A. (1980), An empirical correlation of bedload transport rates in flumes and natural rivers, *Proc. R. Soc. Lond.*, *A372*, 453-473.

Bathurst, J. C. (1985), Flow resistance estimation in mountain rivers, *Journal of Hydraulic Engineering*, *111*(4), 625-643.

Bathurst, J. C. (2007), Effect of coarse surface layer on bed-load transport, *Journal of Hydraulic Engineering (ASCE)*, *133*(11), 1192-1205.

Brown, C. B. (1950), Sediment transportation., in *Engineering Hydraulics*, edited, pp. 769-857, H.Rouse, New York, Wiley.

Buffington, J. M., and D. R. Montgomery (1997), A systematic analysis of eight decades of incipient motion studies, with special reference to gravel-bedded rivers, *Water Resources Research*, *33*(8), 1993-2027.

Camenen, B., and M. Larson (2005), A bedload sediment transport formula for the nearshore *Estuarine, Coastal Shelf Sci*, *63*, 249-260.

Chanson, H. (1999), Sediment transport mechanism. 1Bedload transport in *The hydraulics of open channel flow*, edited by Chanson, Arnold, 338 Euston road, London NW1 3BH, UK.

Chiari, M., and D. Rickenmann (2010), Back-calculation of bedload transport in steep channels with a numerical model, *Earth Surface Processes and Landforms*, *36*(6), 805-815.

Chin, A. (1998), On the stability of step-pool mountain streams, *The Journal of Geology*, *106*, 59-69.

Clayton, A., and J. Pitlick (2007), Persistence of the surface texture of a gravel-bed river during a large flood, *Earth Surface Processes and Landforms*, *33*, 661-673.

Egiazaroff, I. V. (1965), Calculation of nonuniform sediment concentrations, *Journal of the Hydraulics Division (ASCE)*, *HY4*(6), 225-247.

Einstein, H. A. (1950), The bed-load function for sediment transportation in open channel flows*Rep.*, 71 pp, United States Department of Agriculture - Soil Conservation Service, Washington.

Einstein, H. A., and N. Chien (1953), Transport of sediment mixtures with large ranges of grain sizes*Rep.*, 49 pp, MRD Sediment Series No.2, U.S. Army Engineer Division, Missouri River, Corps of Engineers, Omaha, Neb.

Engelund, F., and E. Hansen (1967), A monograph on sediment transport in alluvial streams*Rep.*, 62 pp, Technical University of Denmark.

Ferguson, R. (2007), Flow resistance equations for gravel and boulder bed streams, *Water Resources Research*, *43*(W05427), 1-12.

Gilbert, G. K. (1914), The Transportation of Debris by Running Water*Rep.*, 263 pp, US Geological Survey, Washington Government Printing Office.

Gimenez-Curto, L. A., and M. A. Cornerio (2006), Comment on "Characteristic dimensions of the step-pool bed configuration: an experimental study" by Joanna C.Curran and Peter Wilcock, *Water Resources Research*, *42*.

Grant, G., F. Swanson, and G. Wolman (1990), Pattern and origin of stepped-bed morphology in high-gradient streams, Western Cascades, Oregon, *Geological Society of America Bulletin*, *102*, 340-352.

Grant, G. E. (1997), Critical flow constrains flow hydraulics in mobile-bed streams: A new hypothesis, *Water Resources Research*, *33*(2), 349-358.

Guy, H. P., D. B. Simons, and E. V. Richardson (1966), Summary of alluvial channel data from flume experiments, 1956-61*Rep.*, 96 pp, USGS report n° 462-I.

Hager, W. H. (2005), Du Boys and sediment transport., *J. Hydraul. Res.*, *43*, 227–233.

Hey, R. D. (1979), Flow resistance in gravel bed rivers, *Journal of the Hydraulics Division (ASCE)*, *105*(4), 365-379.

Keulegan, G. B. (1938), Laws of turbulent flow in open channels, *Journal of Research of the National Bureau of Standards*, *21*(Research Paper 1151), 707-741.

Komar, P. D. (1987), selective grain entrainment by a current from a bed of mixed sizes: a reanalysis, *Journal of Sedimentary Petrology*, *57*(6), 203-211.

Kuhnle, R. A. (1992), Fractional transport rates of bedload on Goodwin Creek, in *Dynamics of gravel bed rivers*, edited by P.Billi, R. D. Hey, C. Thorne and P. Tacconi, pp. 141-155, John Wiley & Sons.

Lamb, M. P., W. E. Dietrich, and J.-G. Venditti (2008), Is the critical Shields stress for incipient sediment motion dependent on channel-bed slope?, *J. Geophys. Res.*, *113*(F02008, doi:10.1029/2007JF000831).

Lanzoni, S. (2000), Experiments on bar formation in a straight flume 2. Graded sediment, *Water Resources Research*, *36*(11), 3351.

Lawrence, D. S. L. (1997), Macroscale surface roughness and frictional resistance in overland flow, *Earth Surface Processes and Landforms*, *22*, 365-382.

Lenzi, M. A. (2001), Step-pool evolution in the rio Cordon, northeastern Italy, *Earth Surface Processes and Landforms*, *26*, 991-1008.

Lenzi, M. A., L. Mao, and F. Comiti (2004), Magnitude frequency analysis of bed load data in an Alpine boulder bed stream, *Wat. Resour. Res.*, *40*(W0720).

Lisle, T. E. (1995), Particle size variations between bed load and bed material in natural gravel bed channels, *Water Resources Research*, *31*(4), 1107-1118.

Meyer-Peter, E., and R. Mueller (1948), Formulas for bed-load transport, paper presented at Proceedings 2nd Meeting IAHR, Stockholm.

Milhous, R. T. (1973), Sediment transport in a gravel-bottomed stream, 232 pp, phD thesis, Oregon State University, Corvallis.

Misset, C., A. Recking, C. Legout, N. Valsangkar, N. Bodereau, S. Zanker, A. Poirel, and L. Borgniet (2020a), The dynamics of suspended sediment in a typical Alpine river reach: insight from a seasonal survey, *Water Resour. Res.*

Misset, C., et al. (2020b), Combining multi-physical measurements to quantify bedload transport and morphodynamic interactions in an Alpine braiding river reach, *Geomorphology*.

Molnar, P., A. L. Densmore, B. W. McArdell, J. M. Turowski, and P. Burlando (2010), Analysis of changes in the step-pool morphology and channel profile of a steep mountain stream following a large flood, *Geomorphology*, *124*(1-2), 85-94.

Mueller, E. R., and J. Pitlick (2005), Morphologically based model for bedload transport capacity in a headwater stream, *J. Geophys. Res.*, *110*(F02016), 1-14.

Mueller, E. R., and J. Pitlick (2014), Sediment supply and channel morphology in moutain river systems: 2. Single thread to braided transition, *Journal of Geophysical Research*, *119*, 1516-1554.

Nikora, V. I., D. Goring, I. McEwan, and G. Griffiths (2001), Spatially averaged open-channel flow over rough bed, *Journal of Hydraulic Engineering*, *127*(2), 123-133.

Nikuradse, J. (1933), Strömungsgesetze in rauhen Rohren (Laws of Flow in Rough Pipes), *Forschungsheft Verein Deutscher Ingenieure N°361*.

Nowell, A. R., and M. Church (1979), Turbulent flow in a depth-limited boundary layer, *Journal of Geophysical research*, *84*(C8), 4816-4824.

Parker, G. (1979), Hydraulic geometry of active gravel rivers, *Journal of Hydraulic Engineering (ASCE)*, *105*(9), 1185-1201.

Parker, G. (1990), Surface-based bedload transport relation for gravel rivers, *Journal of Hydraulic Research*, *28*(4), 417-428.

Parker, G. (2009), M.S. Yalin's contribution to bedload transport in rivers: 46 years of hindsight, *Can. J. Civ. Eng.*, *36*, 1579-1586.

Parker, G., and P. C. Klingeman (1982), On why gravel bed streams are paved, *Water Resources Research*, *18*(5), 1409-1423.

Parker, G., P. C. Klingeman, and D. G. McLean (1982), Bedload and size distribution in paved gravel-bed streams, *Journal of the Hydraulics Division (ASCE)*, *108*(HY4), 544-571.

Parker, G., G. Seminara, and L. Solari (2003), Bed load at low Shields stress on arbitrarily sloping beds: Alternative entrainment formulation, *Water Resources Research*, *39*(7), 1183.

Peterson, A. W., and R. F. Howells (1973), A Compendium of Solids Transport Data for Mobile Boundary Channels*Rep.*, Department of Civil Engineering, the University of Alberta.

Petit, F. (1994), Dimensionless critical shear stress evaluation from flume experiments using different gravel beds, *Earth Surface Processes and Landforms*, *19*, 565-576.

Piton, G., and A. Recking (2017), The concept of “travelling bedload” and its consequences for bedload computation in mountain streams, *Geomorphology*.

Piton, G., and A. Recking (2019), Steep Bedload-laden Flows: Near-Critical?, *Journal of Geophysical Research*.

Recking, A. (2009), Theoretical development on the effects of changing flow hydraulics on incipient bedload motion, *Water Resources Research*, *45, W04401*, 16.

Recking, A. (2010), A comparison between flume and field bedload transport data and consequences for surface based bedload transport prediction, *Water Resources Research*, *46*, 1-16.

Recking, A. (2013a), A simple method for calculating reach-averaged bedload transport, *Journal of Hydraulic Engineering*, *139*(1).

Recking, A. (2013b), An analysis of non-linearity effects on bedload transport prediction, *Journal of Geophysical Research - Earth Surface*, *118*, 1-18.

Recking, A. (2016), A Generalized Threshold Model for computing bedload grain size distribution, *Water Resour. Res.*

Recking, A., and J. Pitlick (2013), Shields versus Isbach, *Journal of Hydraulic Engineering*, *139*(1), 1-5.

Recking, A., P. Leduc, F. Liébault, and M. Church (2012), A field investigation of the influence of sediment supply on step-pool morphology and stability, *Geomorphology*, *139-140*, 53-66.

Recking, A., G. Piton, D. Vazquez-Tarrio, and G. Parker (2016), Quantifying the morphological print of bedload transport, *Earth Surface Processes and Landforms*.

Recking, A., P. Frey, A. Paquier, P. Belleudy, and J. Y. Champagne (2008), Feedback between bed load and flow resistance in gravel and cobble bed rivers, *Water Resources Research*, *44*, 21.

Rickenmann, D. (1991), Hyperconcentrated flow and sediment transport at steep slopes, *Journal of Hydraulic Engineering (ASCE)*, *117*(11), 1419-1439.

Rickenmann, D. (2012), Alluvial steep channels: flow resistance, bedload transport and transition to debris flows, in *Gravel Bed Rivers: Processes, Tools, Environment*, edited by M. Church, P. Biron and A. Roy, pp. 386-397, John Wiley & Sons, Chichester, England.

Rickenmann, D., and A. Recking (2011), Evaluation of flow resistance in gravel-bed rivers through a large field dataset, *Water Resources Research*, *47*, 1-22.

Schoklitsch, A. (1962), *Handbuch des Wasserbaus (in German), Springer Verlag (3rd edition)*, Wien.

Shields, A. (1936), Application of similarity principles and turbulence research to bed load movement*Rep.*, US Dept of Agr. , Soil Conservation Service Cooperative Laboratory, California Institute of Technology, Passadena, Calif.

Smart, G. M., and M. N. R. Jaeggi (1983), *Sediment transport on steep slopes*, 89-191 pp., Mitteilungen n°64, Der Versuchsanstalt fuer Wasserbau, Hydrologie und Glaziologie, Eidg. Techn. Hochschule Zuerich, Zurich.

Strickler, K. (1923), Beiträge zur Frage der Geschwindigkeitsformel und der Rauhigkeitszahlen für Ström, Kanäle und geschlossene Leitungen, paper presented at Eidgenössisches Amt für Wasserwirtschaft, N°16, Bern, Switzerland.

Turowski, J. M., E. M. Yager, A. Badoux, D. Rickenmann, and P. Molnar (2009), The impact of exceptional events on erosion, bedload transport and channel stability in a step-pool channel, *Earth Surface Processes and Landforms*, *34*, 1661-1673.

Van Rijn, L. C. (1984), Sediment Transport, Part II: Suspended Load Transport, *Journal of Hydraulic Engineering*, *110*(11), 1613-1641.

Van Rijn, L. C. (1984), Sediment transport, Part I: Bedload transport, *Journal of Hydraulic Engineering*, *110*(10), 14311457.

Vázquez-Tarrío, D., M. Tal, B. Camenen, and H. Piégay (2019), Effects of continuous embankments and successive run-of-the-river dams on bedload transport capacities along the Rhône River, France, *Science of the Total environment*, *658*, 1375-1389.

Whitaker, A. C., and D. F. Potts (2007), Analysis of flow competence in an alluvial gravel bed stream, Dupuyer Creek, Montana, *Water Resources Research*, *43*(W07433), 1-16.

Whitaker, A. C., and D. Potts (2007), Coarse bed load transport in an alluvial gravel bed stream, Dupuyer Creek, Montana, *Earth Surface Processes and Landforms*, *32*(13), 1984-2004.

White, C. M. (1940), The equilibrium of grains on the bed of a stream, *Proc. Roy. Soc.*, *A 174*, 322-338.

Whittaker, J. G., and M. Jaeggi (1982), Origin of step-pool systems in mountain streams, *Journal of the Hydraulics Division*, *108*(HY6), 758-773.

Wiberg, P., and J. D. Smith (1987), Calculation of the critical Shear stress for motion of uniform and heterogeneous sediments, *Water Resources Research*, *23*(8), 1471-1480.

Wiberg, P., and J. D. Smith (1991), Velocity distribution and bed roughness in high-gradient streams, *Water Resources Research*, *27*(8), 825-838.

Wilcock, P. (2001), Toward a practical method for estimating sediment-transport rate in gravel-bed rivers, *Earth Surface Processes and Landforms*, *26*, 1395-1408.

Wilcock, P., J. Pitlick, and Y. Cui (2009), Sediment transport primer, Estimating bed-material transport in gravel-bed rivers*Rep.*, 78 pp, Gen Tech Rep RMRS-GTR-226. Fort Collins, CO: U.S. Department of Agriculture, Forest service, Rocky Mountain Research Station.

Wilcock, P. R. (1993), Critical shear stress of natural sediments, *Journal of Hydraulic Engineering*, *119*(4), 491-505.

Wilcock, P. R., and B. W. Mc Ardell (1997), Partial transport of a sand/gravel sediment, *Water Resources Research*, *33*(1), 235.

Wilcock, P. R., and J. C. Crowe (2003), Surface-based transport model for mixed-size sediment, *Journal of Hydraulic Engineering (ASCE)*, *129*(2), 120-128.

Wilcock, P. R., and B. T. DeTemple (2005), Persistence of armor layers in gravel-bed streams, *Geophysical Research Letter*, *32*(L08402), 1-4.

Wilcock, P. R., S. T. Kenworthy, and J. C. Crowe (2001), Experimental study of the transport of mixed sand and gravel, *Water Resources Research*, *37*(12), 3349.

Williams, G. P. (1970), Flume Width and Water Depth Effects in Sediment Transport Experiments*Rep.*, US Geological Survey.

Wong, M., and G. Parker (2006), Re-analysis and correction of bed load relation of Meyer-Peter and Muller using their own database, *Journal of Hydraulic Engineering*, *132*(11), 1159-1168.

Yu, G.-A., Z.-Y. Wang, K. Zhang, T.-C. Chang, and H. Liu (2009), Effect of incoming sediment on the transport rate of bed load in mountains streams, *International Journal of Sediment Research*, *24*, 260-273.